

ADVANCED ELECTRODE MATERIALS FOR
ELECTROCHEMICAL SUPERCAPACITORS

By

DEEPAK KUMARAPPA ARIYANAYAGAM,

B. E.

ADVANCED ELECTRODE MATERIALS FOR
ELECTROCHEMICAL SUPERCAPACITORS

By

Deepak Kumarappa Ariyanayagam, B. E.

A Thesis

Submitted to the School of Graduate Studies

In Partial Fulfillment of the Requirements

For the Degree

Master of Applied Science

McMaster University

© Copyright by Deepak Kumarappa Ariyanayagam, November 2011

MASTER OF APPLIED SCIENCE (2011) McMaster University

(Materials Science and Engineering)

Hamilton, Ontario

TITLE: Advanced Electrode Materials for Electrochemical
Supercapacitors

AUTHOR: Deepak Kumarappa Ariyanayagam, B.E. (Anna
University, India)

SUPERVISOR: Dr. Igor Zhitomirsky

NUMBER OF PAGES: xii, 99

Abstract

Electrochemical supercapacitors (ES) have become an attractive research interest in advanced power systems and found many applications as an energy storage device in number of areas. The fabrication of advanced electrodes with novel materials and new techniques plays a key part in determining the properties of ES. Conducting polymer polypyrrole (PPY) has been found to be a promising electrode material for ES due to its high pseudo-capacitance and good electrical conductivity.

Polypyrrole (PPY) films were successfully obtained on stainless steel substrates by anodic electropolymerization. Anionic dopants such as 2,6-naphthalenedisulfonic acid disodium salt (NSA), chromotropic acid disodium salt (CHR) and gallic acid were used for the synthesis of PPY. The roles of additives in the electrodeposition process have been discussed. The deposition was performed galvanostatically or potentiodynamically and the electrochemical properties of PPY have been investigated and compared by using different characterization techniques.

The comparison of the experimental data for NSA, CHR and gallic acid showed the influence of aromatic ring and OH groups on the capacitive behaviour of PPY films. Adherent PPY films were obtained from pyrrole solutions containing CHR as dopant. The specific capacitance (SC) increased with increasing pyrrole and dopant concentration in the solutions used for deposition. The PPY films prepared on stainless steel substrates by electropolymerization are promising electrode materials for ES.

Acknowledgement

I hereby sincerely acknowledge the support of many people without whom I would never have been able to complete this thesis.

First, I am greatly thankful to my supervisor, Dr. Igor Zhitomirsky, who has provided me intellectual challenges, constant encouragements and an appropriate research environment throughout my research period.

I would like to thank Chao Shi, who has introduced me to the electrochemical supercapacitors in the beginning of my research.

I would also thank all my group mates in the lab, Xin Pang, Yaohui Wang, Kangming Wu, Yingying Li, Rong Ma, Lijia Yang, Xiaofei Li, Yanchao Sun, Mustafa Ata and Imran Deen for their friendship and for rescuing me whenever I needed help.

Last but not least, my special gratitude to my family for their love and support.

I am very thankful for the financial support from the Natural Science and Engineering Research Council of Canada (NSERC).

Table of Contents

| | |
|--|------|
| Abstract | iii |
| Acknowledgement | iv |
| Table of Contents | v |
| List of Figures | viii |
| List of Tables | xii |
| 1 Introduction..... | 1 |
| 2 Literature Review | 3 |
| 2.1 Energy storage requirement | 3 |
| 2.2 Advantages of supercapacitors compared to other energy storage devices | 3 |
| 2.3 Applications | 6 |
| 2.4 Energy storage mechanisms | 7 |
| 2.4.1 Electrochemical double layer capacitors..... | 7 |
| 2.4.2 Pseudo-capacitors | 9 |
| 2.4.3 Hybrid systems..... | 10 |
| 2.5 Electrode Materials | 11 |
| 2.5.1 High Specific Surface Area Materials | 12 |
| 2.5.2 Pseudocapacitive materials | 18 |
| 2.6 Electrolytes..... | 32 |

| | | |
|-------|--------------------------------------|----|
| 2.6.1 | Aqueous Electrolytes | 33 |
| 2.6.2 | Organic Electrolytes..... | 34 |
| 2.6.3 | Ionic electrolytes..... | 35 |
| 2.7 | Fabrication of CP Electrodes..... | 35 |
| 2.7.1 | Chemical Polymerization..... | 35 |
| 2.7.2 | Electrochemical Polymerization | 36 |
| 2.7.3 | Effect of solvent..... | 38 |
| 2.7.4 | Effect of dopant ions..... | 39 |
| 2.7.5 | Effect of pH..... | 39 |
| 2.7.6 | Effect of temperature | 40 |
| 3 | Objectives | 41 |
| 4 | Approach and methodology..... | 42 |
| 4.1 | Approach | 42 |
| 4.2 | Methodology | 42 |
| 4.2.1 | Dissolution of substrate..... | 42 |
| 4.2.2 | Role of anionic additives | 43 |
| 5 | Experimental Procedures..... | 46 |
| 5.1 | Starting Materials | 46 |
| 5.2 | Experiment Set-up..... | 46 |

| | | |
|-------|--|----|
| 5.3 | Electropolymerization and Electrodeposition of PPY | 46 |
| 5.4 | PPY film Characterization | 48 |
| 5.4.1 | Electrochemical characterization | 48 |
| 5.4.2 | Morphology Characterization | 49 |
| 5.4.3 | Adhesion Test | 49 |
| 6 | Results and Discussions..... | 51 |
| 6.1 | Electropolymerization of PPY doped with CHR | 51 |
| 6.1.1 | Cyclic Voltammogram Electropolymerization of PPY | 51 |
| 6.1.2 | Galvanostatic Electropolymerization of PPY | 52 |
| 6.1.3 | Characterizations of PPY Film | 55 |
| 6.2 | Electropolymerization of PPY doped with gallic acid | 76 |
| 6.2.1 | Potentiodynamic electropolymerization of PPY..... | 76 |
| 6.2.2 | Galvanostatic electropolymerization of PPY | 78 |
| 6.2.3 | Characterization of PPY film deposited using gallic acid | 79 |
| 7 | Conclusions | 86 |
| | References..... | 88 |

List of Figures

| | |
|--|----|
| Figure 2-1 Ragone plot of various energy storage devices [5]. | 5 |
| Figure 2-2 Discharge characteristics of battery, electrostatic capacitor and ES [15]. | 5 |
| Figure 2-3 Schematic diagram of Electrochemical Double Layer Capacitor [49]. | 8 |
| Figure 2-4 Taxonomy of the supercapacitor materials [24]. | 11 |
| Figure 2-5 CV window of carbon blacks as electrode material for EDLC at potential range (1) from -0.5V to +0.5V and (2) from -0.3V to +0.7V [107]. | 13 |
| Figure 2-6 CV curves for activated carbon fibres in 1M NaNO ₃ at (1) 5 mVs ⁻¹ , (2) 15 mVs ⁻¹ , (3) 25 mVs ⁻¹ , (4) 40 mVs ⁻¹ and (5) 50 mVs ⁻¹ [106]. | 14 |
| Figure 2-7 Schematic diagram of the pore size network of an activated carbon [25]. | 15 |
| Figure 2-8 Cyclic voltammogram of carbon aerogel electrodes with different resorcinol(R)/catalyst(C) ratio [108]. | 16 |
| Figure 2-9 Schematic diagrams of (A) SWCNT and (B) MWCNT [26]. | 17 |
| Figure 2-10 Voltammetry characteristics of a capacitor built from carbon nanotubes obtained by decomposition of acetylene at 700° C on Co/SiO ₂ 6M KOH, 1 mV/s [109]. | 18 |
| Figure 2-11 Cyclic voltammogram of ruthenium oxide [34]. | 20 |
| Figure 2-12 Cyclic voltammogram of cobalt oxide [37]. | 21 |
| Figure 2-13 Cyclic voltammogram of nickel oxide [40]. | 22 |
| Figure 2-14 Cyclic voltammogram of manganese oxide [48]. | 23 |
| Figure 2-15 Charge storage mechanism of conducting polymer electrodes, (a) p-type and (b) n-type [45]. | 24 |
| Figure 2-16 Chemical structure of common conducting polymers [93]. | 26 |

| | |
|---|----|
| Figure 2-17 Non-degenerate ground state configurations and charge carrier defects of PPY [98]. | 27 |
| Figure 2-18 Cyclic voltammograms of pure PPY and PPY-CNT composite at scan rate of 20 mV/s [50]. | 31 |
| Figure 2-19 Cyclic voltammograms of PPY, MnO ₂ and PPY-MnO ₂ at a scan rate of..... | 32 |
| Figure 2-20 Mechanism of electropolymerization of PPY [62]. | 37 |
| Figure 4-1 Chronopotentiometry curve for formation of PPY coating on steel in the solution of pH 1.4 at current density of 0.56 mA cm ⁻² [64]. | 43 |
| Figure 4-2 Chemical structure and possible complexation on metal oxides of | 44 |
| Figure 5-1 Schematic representation of experimental set-up in electrodeposition. | 47 |
| Figure 6-1 Cyclic voltammograms at (a) 1 st cycle, (b) 2 nd cycle, (c) 3 rd cycle and (d) 10 th cycle for stainless steel electrode in 50 mM pyrrole solution containing 5 mM CHR at a scan rate of 20 mV s ⁻¹ . | 51 |
| Figure 6-2 The chemical structure of (a) 2,6-Naphthalenedisulfonic acid, disodium salt (NSA) and (b) Chromotropic acid disodium salt dihydrate (CHR). | 53 |
| Figure 6-3 Potential versus time curves for galvanostatic deposition of PPY at a current density of 1mA cm ⁻² from 50 mM pyrrole solution in presence of (a) 5 mM NSA and (b) 5 mM CHR. | 54 |
| Figure 6-4 Film mass versus deposition time for films deposited from 50 mM pyrrole solution containing 5 mM CHR at a current density of 1 mA cm ⁻² . | 55 |
| Figure 6-5 SEM images of surface of PPY film doped with CHR on stainless steel shown at a (a) low magnification and (b) high magnification. | 57 |

| | |
|---|----|
| Figure 6-6 Cyclic voltammograms at scan rates of (a) 2, (b) 5 and (c) 10 mV s^{-1} in | 59 |
| Figure 6-7 Cyclic voltammograms in 0.5 M Na_2SO_4 solution for 0.15 mg cm^{-2} PPY film, prepared from the solution containing (a) 50 mM pyrrole and 5 mM CHR and (b) 100 mM pyrrole and 5 mM CHR..... | 60 |
| Figure 6-8 SEM images of films prepared from 150 mM pyrrole solution containing (a) 5, (b) 15 and (c) 50 mM CHR..... | 63 |
| Figure 6-9 Specific capacitance versus scan rate for 0.1 mg cm^{-2} films prepared at current density of 1 mA cm^{-2} from (a) 50 mM pyrrole and 5mM CHR, (b) 100 mM pyrrole and 5mM CHR, (c) 150 mM pyrrole and 5 mM CHR , (d) 150 mM pyrrole and 15 mM CHR and (e) 150 mM pyrrole and 50 mM CHR. | 65 |
| Figure 6-10 Specific capacitance at scan rates of (a) 2 and (b) 100 mV s^{-1} versus mass of the films prepared from 100 mM pyrrole solutions containing 5 mM CHR. | 66 |
| Figure 6-11 Cyclic voltammograms in 0.5 M Na_2SO_4 solution for PPY film, prepared from the solution containing 150 mM pyrrole and 5 mM CHR of film mass of | 67 |
| Figure 6-12 Specific capacitance versus scan rate for films of mass | 68 |
| Figure 6-13 Nyquist plots for the 0.1 mg cm^{-2} films prepared at a current density of..... | 69 |
| Figure 6-14 Nyquist plots for the 0.1 mg cm^{-2} films prepared at a current density of..... | 70 |
| Figure 6-15 Equivalent circuit model for PPY electrode in a 0.5 M Na_2SO_4 electrolyte. . | 72 |
| Figure 6-16 Nyquist plots of complex impedance $Z = Z' - iZ''$ for (a) 0.18 and..... | 73 |
| Figure 6-17 CV of the PPY film of mass 0.15 mg cm^{-2} recorded in the (a)1 st and (b)1000 th potential cycle at a scan rate of 50 mV s^{-1} in 0.5M Na_2SO_4 electrolyte solution. | 74 |

| | |
|--|----|
| Figure 6-18 Specific capacitance versus cycle number at a scan rate of 50 mV s^{-1} for 0.15 mg cm^{-2} film prepared from the solution containing 150 mM pyrrole | 75 |
| Figure 6-19 Cyclic voltammograms at (a) 1 st cycle, (b) 2 nd cycle, (c) 3 rd cycle, (d) 4 th cycle and (e) 10 th cycle for stainless steel electrode in 50 mM pyrrole solution containing 5 mM Gallic acid at a scan rate of 20 mV s^{-1} | 77 |
| Figure 6-20 Potential versus time curves for galvanostatic deposition of PPY at a current density of 1 mA cm^{-2} from 50 mM pyrrole solution in presence of 5 mM gallic acid. | 79 |
| Figure 6-21 Film mass versus deposition time for films deposited from 250 mM pyrrole solution containing 50 mM gallic acid at a current density of 1 mA cm^{-2} | 80 |
| Figure 6-22 Cyclic voltammograms at scan rates of (a) 2, (b) 5 and (c) 10 mV s^{-1} for 0.083 mg cm^{-2} PPY film, prepared from the solution containing 250 mM pyrrole and 50 mM CHR | 82 |
| Figure 6-23 Cyclic voltammograms at scan rates of (a) 2, (b) 5 and (c) 10 mV s^{-1} for 0.116 mg cm^{-2} PPY film, prepared from the solution containing 250 mM pyrrole and 50 mM CHR | 82 |
| Figure 6-24 Cyclic voltammograms at scan rates of (a) 2, (b) 5 and (c) 10 mV s^{-1} in 0.5 M Na_2SO_4 solution for 0.188 mg cm^{-2} PPY film, prepared from the solution containing 250 mM pyrrole and 50 mM CHR | 83 |
| Figure 6-25 Specific capacitance versus scan rate for films of mass | 84 |
| Figure 6-26 Nyquist plots for the films prepared at a current density of 1 mA cm^{-2} from the solution containing 50 mM Gallic acid and 250 mM Pyrrole with a film mass of (a) 0.083 mg cm^{-2} , (b) 0.116 mg cm^{-2} and (c) 0.188 mg cm^{-2} | 85 |

List of Tables

| | |
|---|----|
| Table 2-1 EDLC and pseudo-capacitance compared [15]..... | 10 |
| Table 2-2 Comparison of aqueous electrolyte and organic electrolyte [56]..... | 33 |
| Table 2-3 Comparison of chemical and electrochemical polymerization [59]..... | 38 |
| Table 5-1 Classification of Adhesion Test Results..... | 50 |

1 Introduction

Energy consumption is one of the major challenges that our society faces in recent days. An ideal energy storage device should provide high energy in short time i.e. high power density and also store and deliver large amount of energy i.e. high energy density. Among all other energy storage devices, electrochemical supercapacitors (ES) exhibit higher power density than batteries and solar cells and higher energy density than conventional capacitors because of unique charge storage mechanisms.

On the basis of charge storage mechanisms, ES can be categorized into two types, (i) electrochemical double-layer capacitors in which the capacitance evolves from the charge separation at the electrode and electrolyte interface and (ii) pseudocapacitors which utilize the charge transfer pseudo-capacitance arising from reversible Faradaic reaction occurring at the electrode surface. Hence the electrode material is an important aspect in the capacitive behaviour of ES. The common electrode materials which gained interest recently are high surface area carbon, transition metal oxides and conducting polymers.

Conducting polymers attracted much attention as electrode materials because of their high electrical conductivity which reduces the internal resistance and high pseudo-capacitance. Polypyrrole (PPY) is a promising conducting polymer for electrochemical energy storage because of its high capacitance and good chemical stability. High flexibility and ease fabrication are important advantages of PPY films.

In this research, electrochemical polymerization method has been developed for the fabrication of PPY films on stainless steel substrates. The new approach is based on the use of new anionic additives, which prevented the substrate dissolution during electropolymerization, reduced the electropolymerization potential and provided charge compensation during electropolymerization. It is an attractive method because the polymerization of pyrrole and deposition of a film on a metal substrate happens in a single step, which restricts the dissolution of metal during the process. PPY films were deposited on the metal stainless steel substrates in an easy way from the solution containing pyrrole and anionic additives. Anionic additives play a vital role in the fabrication of PPY films with desired microstructure, morphology, physical and electrochemical properties. Gallic acid and chromotropic acid disodium salt dihydrate (CHR) were chosen as the anionic additives to deposit PPY films on stainless steel substrates. The influence of OH groups of these additives on their adsorption on stainless steel and electrochemical behaviour was observed. Uniform PPY films were obtained on the low cost stainless steel substrates. The film showed good capacitive behaviour which was investigated by several electrochemical techniques. The PPY films deposited on stainless steel substrates are promising materials for application in ES using low cost stainless steel current collectors.

2 Literature Review

2.1 Energy storage requirement

As the depletion of fossil fuels increased, the consumption of fossil fuels caused harmful effects on environment. The attention of researchers is focused on the use of renewable and clean energy sources which can be an alternative for fossil fuels [1]. Various devices are under development for storing energy, such as batteries, conventional capacitors, fuel cells etc. ES have gained more interest in recent days.

2.2 Advantages of supercapacitors compared to other energy storage devices

Energy storage devices such as conventional capacitors, batteries, fuel cells, ES have their unique energy storage mechanisms. The charge/discharge behaviour and performance are determined by the way they store energy. In conventional capacitors, energy is stored electrostatically as positive and negative charges on the plates [2]. In batteries, the storage comes as a result of net chemical reaction between electrode and electrolyte [3]. In fuel cells, the storage is based on the oxidation reaction that occurs at the catalytic electrodes [4]. In case of ES, storage is achieved as the result of Faradic electrosorption or redox reaction at the electrodes [2].

The performance of an energy storage device is determined by two key parameters, (i) energy density, which is the amount of energy stored per unit mass and can be expressed by the equation:

$$w = \frac{1}{2} C V^2 \quad (2-1)$$

where, C is the specific capacitance. V is the voltage. (ii) Power density which is the amount of energy delivered per unit mass and can be expressed by the equation:

$$P_{max} = \frac{1}{4R_s} V_i^2 \quad (2-2)$$

Where R_s is the equivalent series resistance (ESR) and V_i is the initial voltage. Based on the power and energy density, the performance of the energy storage devices can be expressed by Ragone plot as shown in Figure 2-1.

It can be noted that the batteries and fuel cells can provide very high energy density, but with very low power density. Meanwhile, the conventional capacitors although possess high power density, couldn't offer high energy density to meet requirement for long duration applications.

Due to the large surface area of the electrodes in ES compared to conventional capacitors, ES exhibit higher energy density than that of conventional capacitors. ES exhibits high power density compared to batteries and fuel cells. Since the electrode of ES doesn't undergo any chemical phase and composition change during the charge/discharge process, ES shows high cyclic stability and reversibility when compared to batteries and fuel cells. Also ES can be used in temperature range of -30°C to $+60^\circ \text{C}$ but the batteries can be operated in narrow temperature range [6].

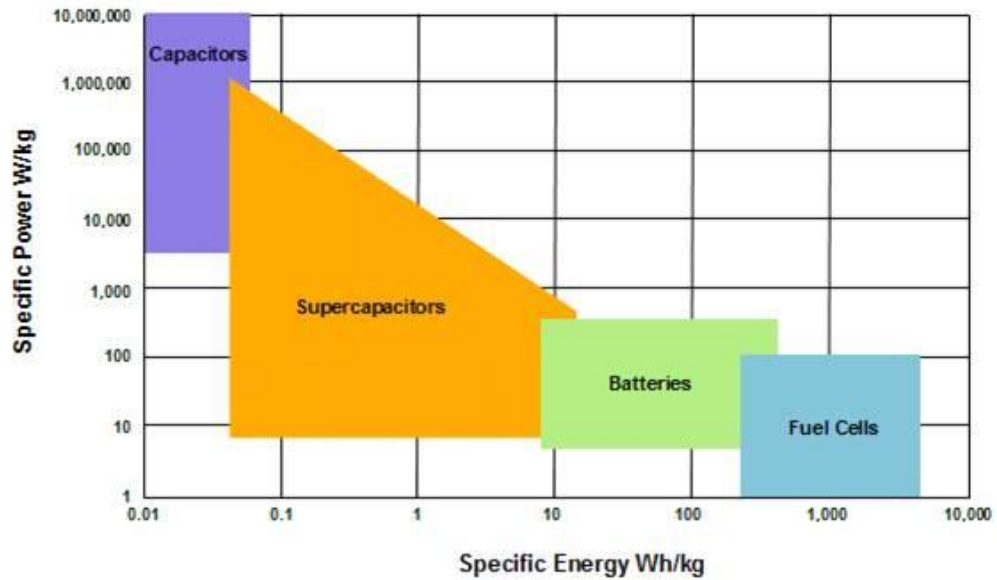


Figure 2-1 Ragone plot of various energy storage devices [5].

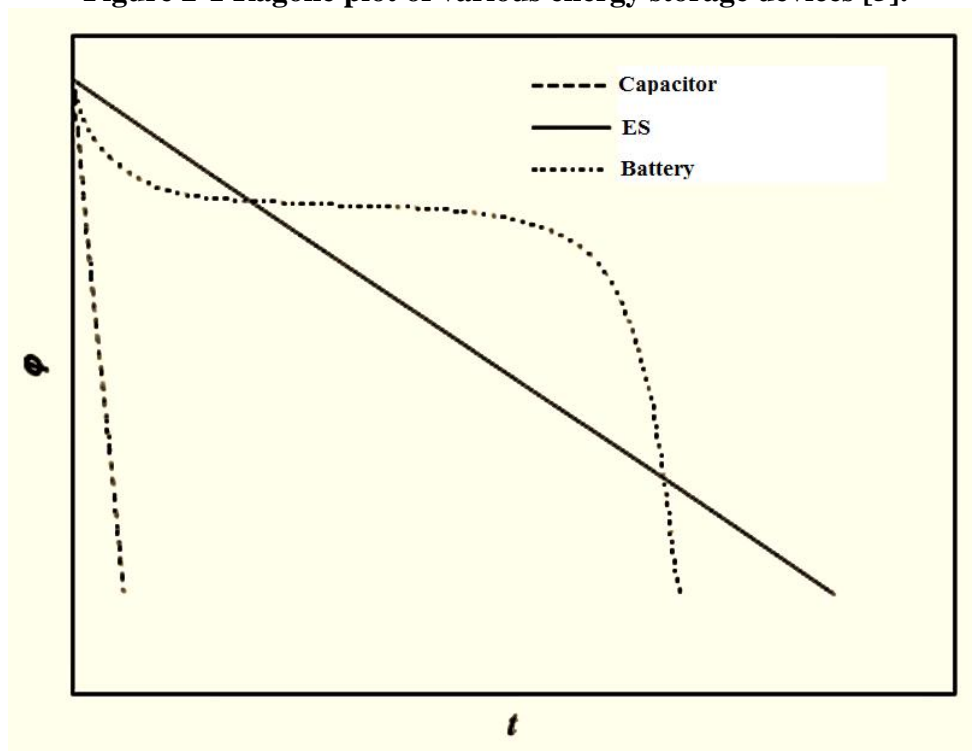


Figure 2-2 Discharge characteristics of battery, electrostatic capacitor and ES [15].

Figure 2-2 shows the comparison of constant current discharge curves of battery, electrostatic capacitor and ES. For battery, the voltage keeps in constant and hence exhibits a discharge plateau in the curve. Linear decrease of voltage with discharge time was observed for capacitor and ES. However, conventional capacitors exhibit better charge-discharge behaviour than that of ES. At constant current, there is a linear relationship between voltage and time of discharge for the ES [15].

The key factor that restricts the ES to be used in the market is relatively high capital cost. The need for high energy density is another limitation. Therefore, there is a high demand in fabricating high power and energy density ES using economically reasonable methods [7].

2.3 Applications

The applications of ES can be categorized into three types, such as energy back up, main and alternating power sources [8]. In case of energy back up applications, ES are connected parallel with a main power source such as battery. So despite of power outages due to turn-off of main power source, voltage drop, contact problems, shock etc., the supercapacitors can still provide energy to the system. This is where the largest part of supercapacitors is used in commercial market to act as back-up sources for memories, microcomputers, system boards and clocks.

As a result of significant increase in energy and power densities due to recent research, supercapacitors can also be used as main power source in various applications such as small portable electronics, transportation and industrial equipment. In case of

electric vehicles, supercapacitors serve as an ideal power source as they can provide high energy efficiency, high power density and ability to recover the energy loss during braking [9,10]. Although batteries and fuel cells serve as energy storage devices for these electric vehicles, they lag in providing power in short time for acceleration and hill climbing. Since supercapacitors have the ability of fast charge/discharge and provide regenerative braking which reduces 15% of fuel consumption [11], they are combined with batteries or fuel cells to meet the above requirement.

2.4 Energy storage mechanisms

2.4.1 Electrochemical double layer capacitors

An electrochemical double layer capacitor (EDLC) has two electrodes immersed in an electrolyte with a separator between the electrodes. Electric charge is accumulated electrostatically on either side of the electrode/electrolyte interface which leads to the formation of electrical double layer [2,3,12].

The capacitance of EDLC can be calculated by the equation:

$$C_{dl} = \frac{\epsilon_r \epsilon_0 A}{d} \quad (2-3)$$

where ϵ_r is the relative dielectric constant in the double layer, ϵ_0 is the permittivity of free space, A is the surface area of the electrode and d is the thickness of the double layer.

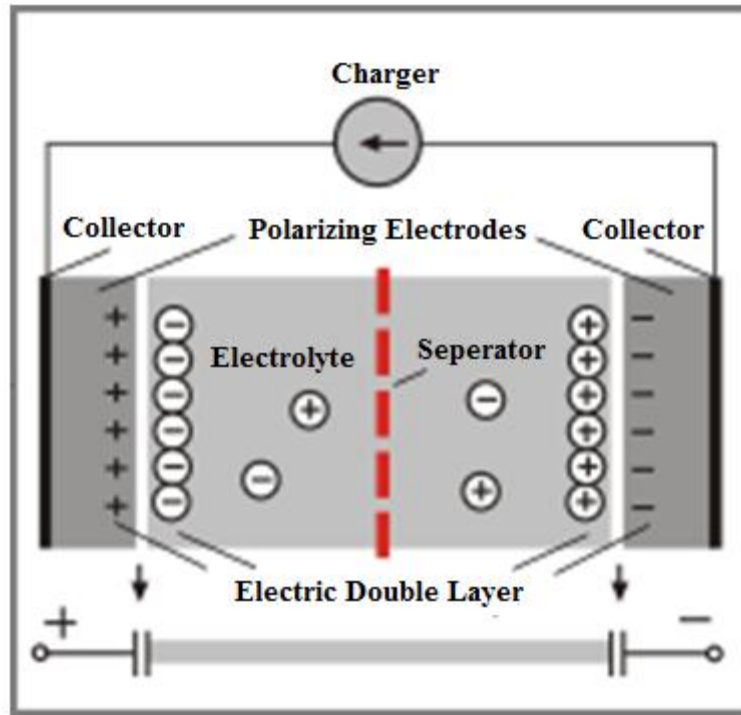


Figure 2-3 Schematic diagram of Electrochemical Double Layer Capacitor [49].

The thickness of the double layer which is in angstrom scale is relatively smaller than the distance of separation between the plates in conventional capacitors which is usually in micrometer scale. When high surface area materials are used as electrodes, the capacitance value of EDLC can be increased by several orders of magnitude, compared to conventional capacitors [2,13]. Since there is no charge transfer occurs across the interface during the charge storage process (non-Faradaic), there is no chemical or compositional change takes place in the system. Therefore a very high degree of reversibility in repetitive charge/discharge process and long cycle life can be attained in EDLC [3].

2.4.2 Pseudo-capacitors

In pseudo-capacitors energy storage is mainly because of the fast and reversible reactions occurring on the electrode surface [2]. The important processes that are responsible for the pseudo-capacitance are: (i) surface adsorption of ions from the electrolyte, (ii) redox reactions involving ions from the electrolyte and (iii) doping and undoping of active conducting polymers in the electrode [12]. The surface area of the electrode plays a vital role in the first two of above processes, whereas the third process which involves conducting polymer is less dependent on surface area as it is a bulk process. However, high surface area with micro-pores promotes the ion access to the electrode material [12]. The pseudo-capacitance can be expressed by the equation:

$$C = \frac{Q_{tot}}{V_{tot}} \quad (2-4)$$

Where Q_{tot} is the total charge and V_{tot} is the voltage change for a charge or discharge of the electrode.

In a supercapacitor system, both the storage mechanism of EDLC and pseudo-capacitor are observed simultaneously even though one of them dominates over the other [14]. The capacitance of the pseudo-capacitors is 10-100 times higher than that of a carbon double layer capacitor [13]. The comparison of EDLC and pseudo-capacitor is shown in the table [15].

Table 2-1 EDLC and pseudo-capacitance compared [15].

| | Double-layer capacitance | Pseudo-capacitance |
|----------|---|---|
| 1 | Non Faradaic | Involves Faradaic process |
| 2 | 20–50 $\mu\text{F cm}^{-2}$ | 2000 $\mu\text{F cm}^{-2}$ for single-state process; 200–500 F cm^{-2} for multi-state, overlapping processes |
| 3 | C fairly constant with potential, except through the point of zero charge (p.z.c.) | C fairly constant with potential for RuO_2 ; for single-state process, exhibits marked maximum |
| 4 | Highly reversible charging/discharging | Quite reversible but has intrinsic electrode-kinetic rate limitation determined by potential-dependent faradaic leakage resistance (R_f). |
| 5 | Has restricted voltage range (in contrast to non-electrochemical electrostatic capacitor) | Has restricted voltage range |
| 6 | Exhibits mirror-image voltammograms | Exhibits mirror-image voltammograms |

2.4.3 Hybrid systems

Hybrid capacitors combine Faradaic and non-Faradaic process to store charge. They improve the merits and minimize the demerits that exist in EDLCs and pseudo-capacitors. Therefore, high energy and power densities than those for EDLCs can be attained with better cyclic stability and affordability than those of pseudo-capacitors [16]. The combined utilization of double layer electrode along with pseudocapacitance electrode which are charged in two different modes is the principle behind the hybrid system. The higher maximum operating voltage and the lower equivalent series

resistance are additional beneficial factors which significantly improve the performance of supercapacitors.

2.5 Electrode Materials

On the basis of electrode materials used, ES can be classified into three types, (i) high specific area materials which utilise double layer capacitance, (ii) redox pseudo-capacitive materials and (iii) composite materials. Figure 2-4 shows various electrode materials used under each category.

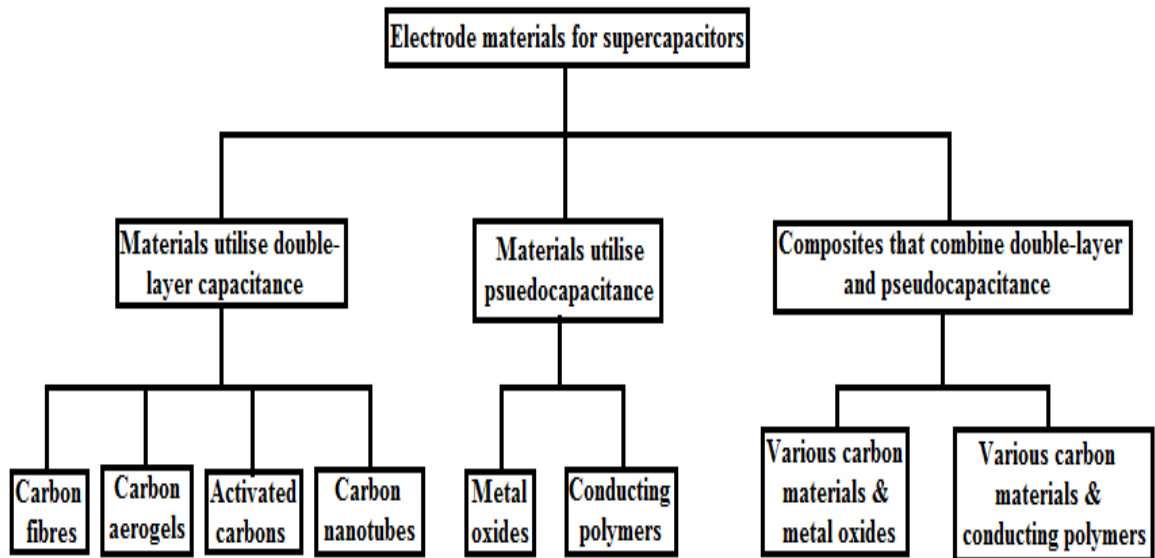


Figure 2-4 Taxonomy of the supercapacitor materials [24].

2.5.1 High Specific Surface Area Materials

Carbon materials in different forms such as carbon fibres, carbon aerogels, activated carbons and carbon nanotubes are most commonly used high specific area electrode materials for ES. These materials exhibit various attractive physical and chemical properties such as high conductivity, high surface area, high temperature stability, good corrosion resistance, high porosity, easy processability and good compatibility in composite materials and relatively low cost [3].

2.5.1.1 Carbon blacks

Carbon blacks are commonly used as the filling materials in electrodes of battery and supercapacitors [102]. Carbon blacks particles are spherical of colloidal size. Carbon blacks are prepared by partial combustion or thermal decomposition of hydrocarbons in the gas phase [103,104]. Carbon blacks have comparatively more accessible surface than other forms of high surface area carbons. High conductivity, high porosity, small particle size and chemically clean surface are attractive properties of carbon blacks. Optimum loading of carbon blacks in EDLC, increases conductivity and surface area which improves the performance of EDLC [3]. The specific capacitance of carbon blacks EDLC is about 250 Fg^{-1} [105]. Cyclic voltammogram of EDLC containing carbon blacks is shown in Figure 2-5.

Carbon blacks have low compact density. For the fabrication of stable electrode, high concentration of binder is required which increases the electrical resistance.

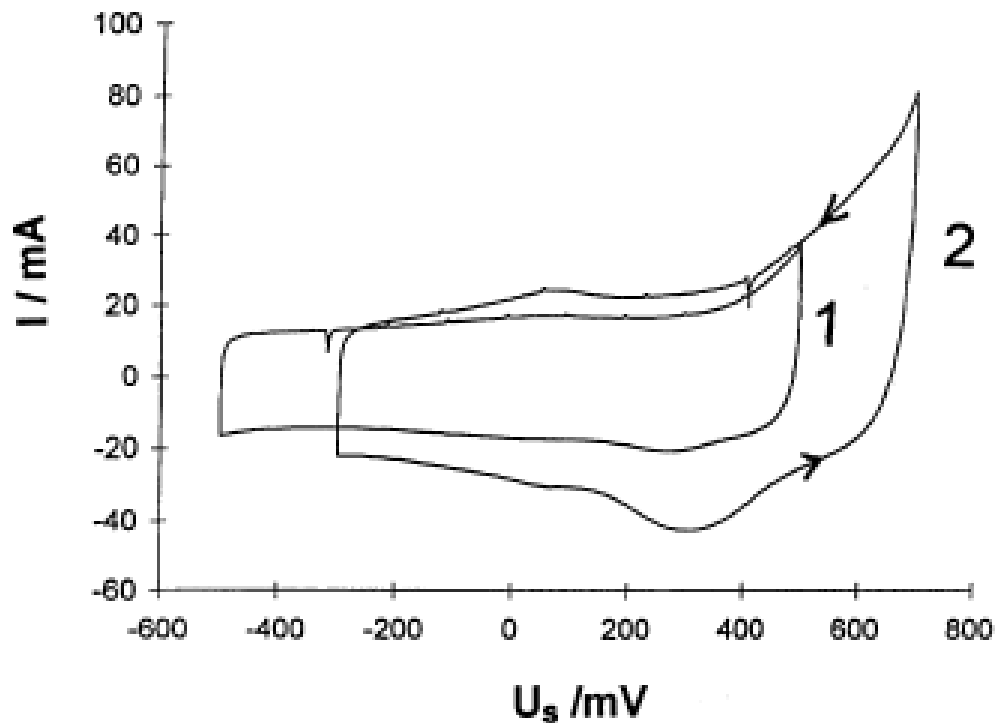


Figure 2-5 CV window of carbon blacks as electrode material for EDLC at potential range (1) from -0.5V to +0.5V and (2) from -0.3V to +0.7V [107].

2.5.1.2 Carbon fibres

Activated carbon fibres are attractive electrode materials for EDLCs since adsorption capacities and adsorption rates of high magnitude can be achieved. The manufacturing process and precursor determine the quality of carbon fibres. The carbon fibres are produced from thermosetting organic materials such as cellulose, phenolic resins, polyacrylonitrile and pitch-based materials. The carbon fibres are prepared by the extrusion process of precursor material through a die or spinnerets and then drawing of the extrudant into thin fibres, which are activated in an oxidising environment. The

diameter of these activated carbon fibres will be in the range of 10 μm . Good accessibility to active sites is provided by the pores that are largely situated at the surface of the fibre. High adsorption capacities and adsorption rates are exhibited by activated carbon fibres. Carbon fibres are woven into carbon clothes and used as electrode materials [106]. Cyclic voltammogram of activated carbon fibres is shown in Figure 2-6, demonstrates excellent capacitive behaviour.

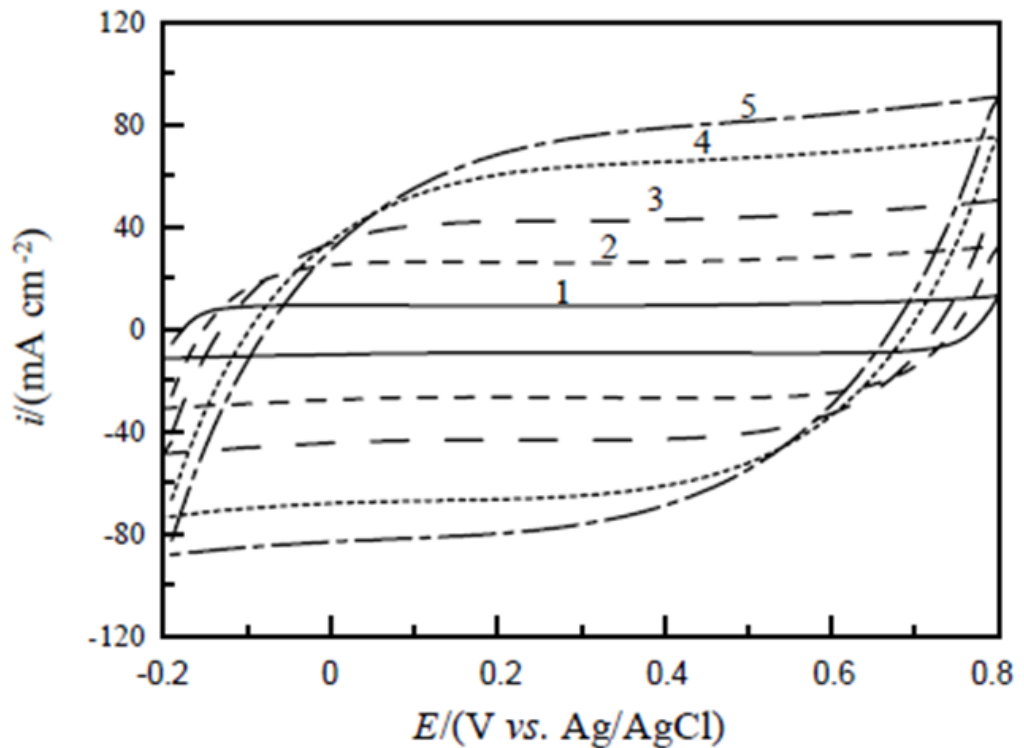


Figure 2-6 CV curves for activated carbon fibres in 1M NaNO₃ at (1) 5 mVs⁻¹, (2) 15 mVs⁻¹, (3) 25 mVs⁻¹, (4) 40 mVs⁻¹ and (5) 50 mVs⁻¹ [106].

Since carbon clothes possess high surface area, high capacitance has been observed. The contact resistance between the individual fibres is high and the cost of

activated carbon fibres is relatively high compared to the other carbon powder products [17].

2.5.1.3 Activated carbons

Activated carbons are produced by thermal or chemical treatment of carbonaceous materials in order to increase their surface area. The porous structure of the activated carbon consists of micropores (diameter < 2 nm), mesopores (diameter from 2 – 50 nm) and macropores (diameter > 50 nm) as represented in the Figure 2-7. Empirical evidence suggests that not all of the high surface area contributes to the capacitance although it is directly proportional to surface area. Smaller micropores cannot support the diffusion of electrolyte ions into them, hence preventing the contribution of some pores for charge storage [3]. Activated carbon is widely used in EDLCs as it is less expensive than other carbon based materials.

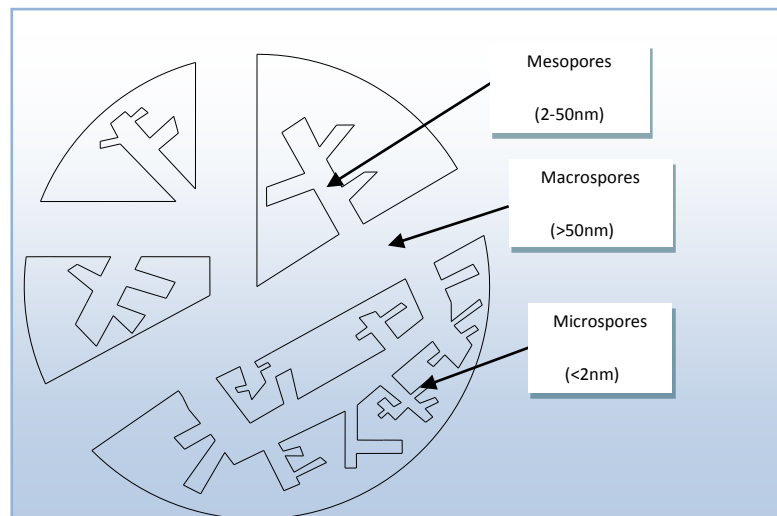


Figure 2-7 Schematic diagram of the pore size network of an activated carbon [25].

2.5.1.4 Carbon aerogels

Carbon aerogels are produced by the pyrolysis of organic aerogels and synthesized by the poly-condensation of resorcinol and formaldehyde and subsequent pyrolysis [17]. Carbon aerogels exhibit good electrical conductivity, high surface area, high density and uniformity in pore size between 2 – 50 nm. They can also be produced as monoliths, composites, thin films, powders or micro-spheres. By means of different activation methods such as thermal activation, electrochemical activation and chemical vapour impregnation, the surface area of aerogels can be increased [3, 17, 18]. Carbon aerogels produced by polycondensation of resorcinol with formaldehyde and sodium carbonate as catalyst, provided specific capacitance of 110 F g^{-1} [108].

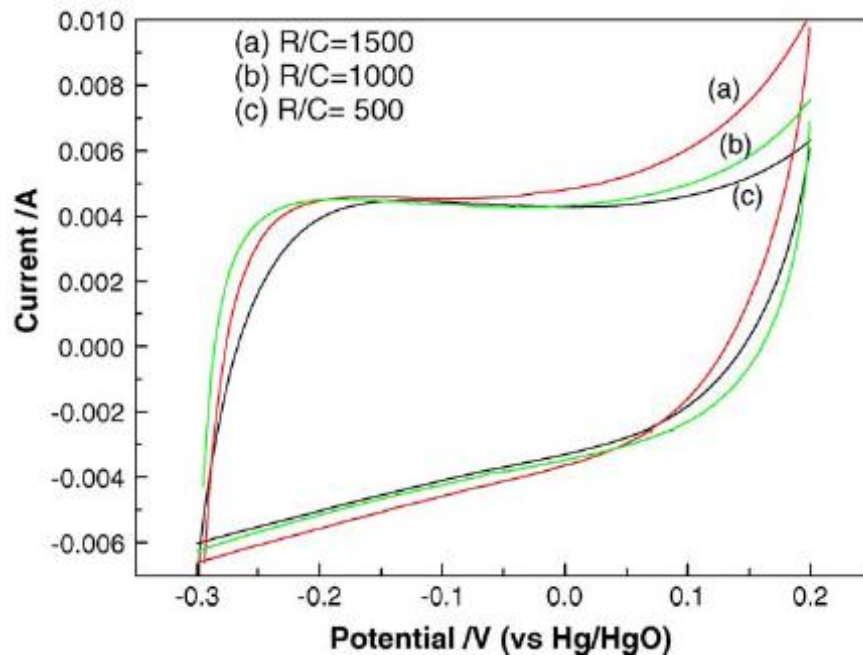


Figure 2-8 Cyclic voltammogram of carbon aerogel electrodes with different resorcinol(R)/catalyst(C) ratio [108].

2.5.1.5 Carbon nanotubes

Carbon nanotubes (CNTs) are produced by catalytic decomposition of hydrocarbons. Based on the nanoscale tubular morphology, CNTs are categorized into (i) single-walled CNTs (SWNTs) and (ii) multi-walled CNTs (MWNTs) [19, 20]. The surface area of CNTs is relatively smaller than that of activated carbons, the specific capacitance was found to be from 15 to 80 Fg^{-1} . CNT shows ideal capacitive behaviour in cyclic voltammetry as shown in the Figure 2-10 [109]. The surface texture of CNTs can be altered and additional functionality can be included by means of oxidative treatment, the specific capacitance can be increased to 130 F g^{-1} [21,22]. On further chemical activation with potassium hydroxide, the capacitance can be increased twice than that of regular CNTs [23].

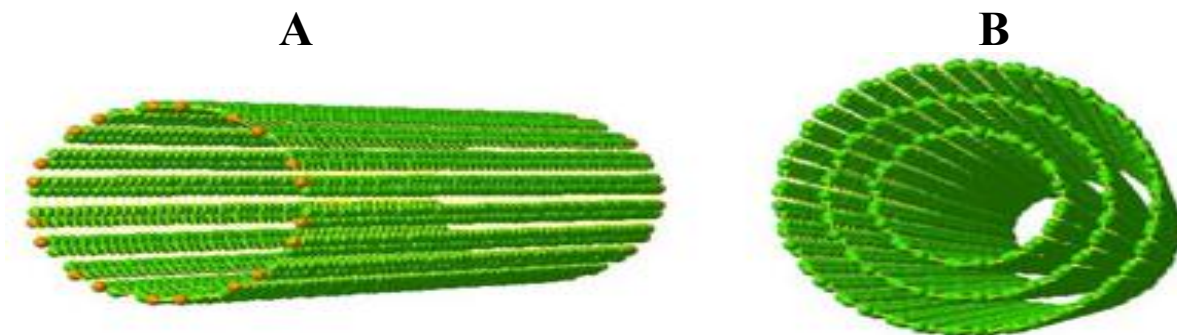


Figure 2-9 Schematic diagrams of (A) SWCNT and (B) MWCNT [26].

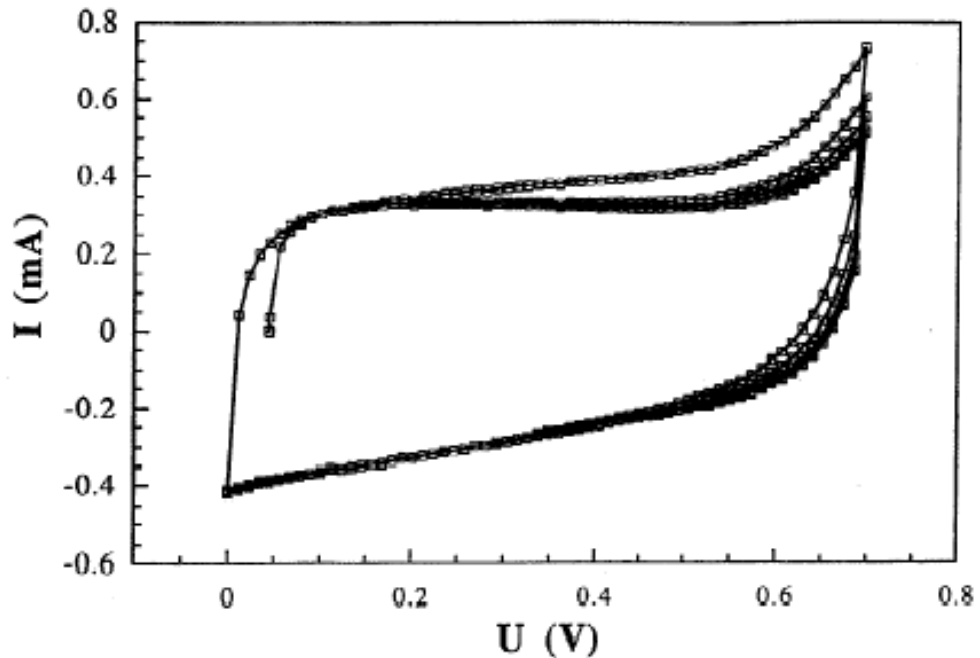


Figure 2-10 Voltammetry characteristics of a capacitor built from carbon nanotubes obtained by decomposition of acetylene at 700° C on Co/SiO₂ 6M KOH, 1 mV/s [109].

Since CNTs possess unique pore structure characteristics like high strength, good electrical conductivity, electrolyte accessibility, chemical and thermal stability, they are considered as promising electrode materials for ES.

2.5.2 Pseudocapacitive materials

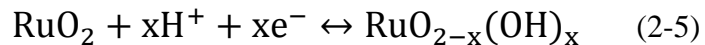
Fast reversible redox reactions occurring at the surface make the pseudocapacitive materials such as transition metal oxides and conducting polymers as promising electrode materials for ES. Specific capacitance of these materials is significantly larger than that of the carbon materials.

2.5.2.1 Transition metal oxides

Metal oxides such as RuO₂, NiO, Co₃O₄, MnO₂ etc. have been widely investigated for electrode materials for ES because they possess high specific capacitance at low resistance. Capacitive behaviour of some metal oxide materials is discussed in the following sections.

2.5.2.1.1 Ruthenium oxide

Using the fast and reversible electron transfer accompanied by an electro-adsorption of proton on the surface, ruthenium oxide achieves a high capacitance in acidic environment. The redox reaction occurring at the surface of the material can be expressed as [27]:



High energy and power densities are achieved when RuO₂ is used as an electrode material because of its low equivalent series resistance (ESR). RuO₂ provides high conductivity, long cycle life and good electrochemical reversibility [28-33]. Cyclic voltammogram of RuO₂ exhibits mirror-image (Fig 2-11) [34], indicating ideal capacitive behaviour. The specific capacitance of hydrous RuO₂ in sulphuric acid was 750 Fg⁻¹ which is much higher than that for anhydrous RuO₂ [27]. Besides these advantages, the utilisation of RuO₂ as electrode material is limited due to its high cost.

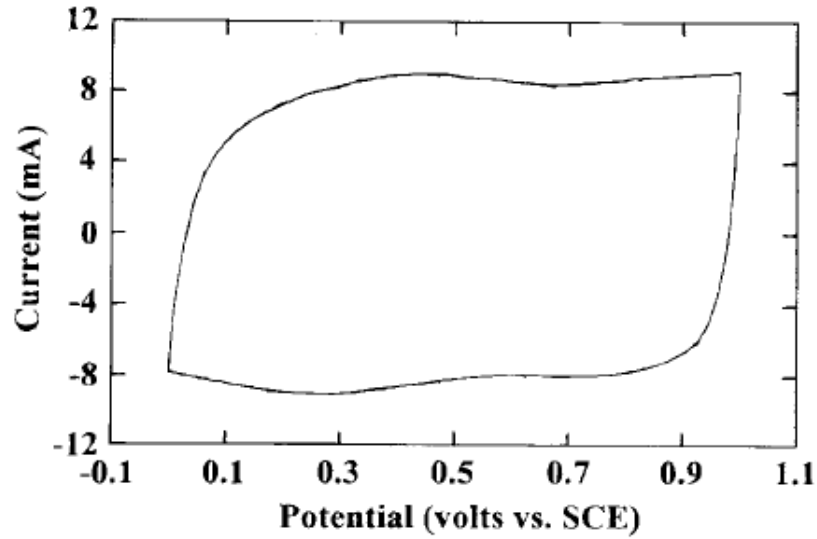
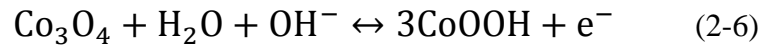


Figure 2-11 Cyclic voltammogram of ruthenium oxide [34].

2.5.2.1.2 Cobalt oxide

Cobalt oxide is considered as a promising electrode material for ES. The charge storage mechanism can be expressed as [35]:



The above mechanism varies with the heat treatment temperature of cobalt oxide as it undergoes phase changes [36]. Cobalt oxide electrodes possess a capacitance value of 164 F g^{-1} . Since cobalt oxide materials show capacitive behaviour in negative voltage range [36,37], they can be coupled with other oxide materials as positive electrode in devices with asymmetric electrode design.

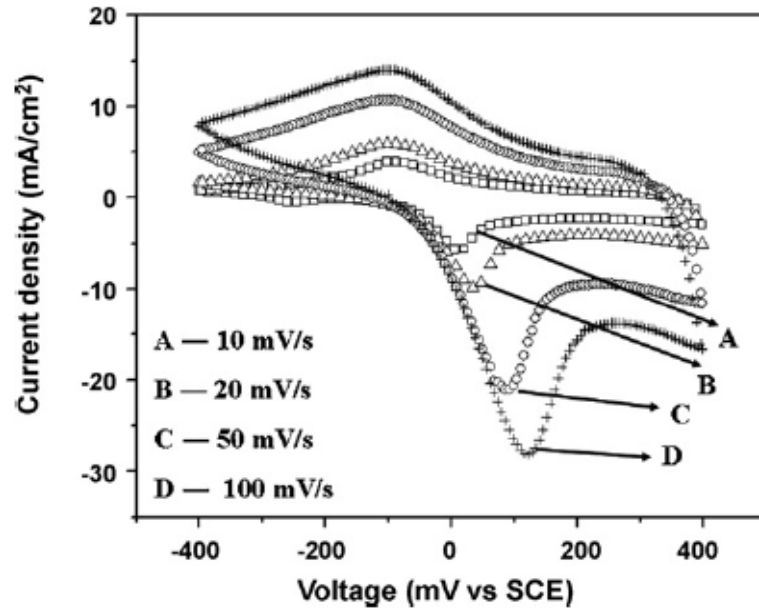
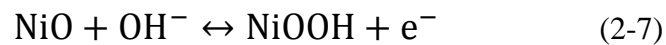


Figure 2-12 Cyclic voltammogram of cobalt oxide [37].

2.5.2.1.3 Nickel oxide

Nickel oxides films are produced by sol-gel techniques for electrode materials for ES [38]. Specific capacitance of about 256 F g^{-1} is obtained. Electrochemical precipitation techniques were developed to prepare nickel oxide films. They are relatively cheaper and more controllable than sol-gel techniques [39]. Charge storage mechanism of nickel oxide can be expressed as [40]:



The major disadvantages of nickel oxide films are (i) they exhibit low capacitance, (ii) voltage window is small and (iii) cyclic voltammogram shows that the current-potential response is potential dependent (Figure 2-13) [40] which is in converse to the behaviour of ideal capacitor.

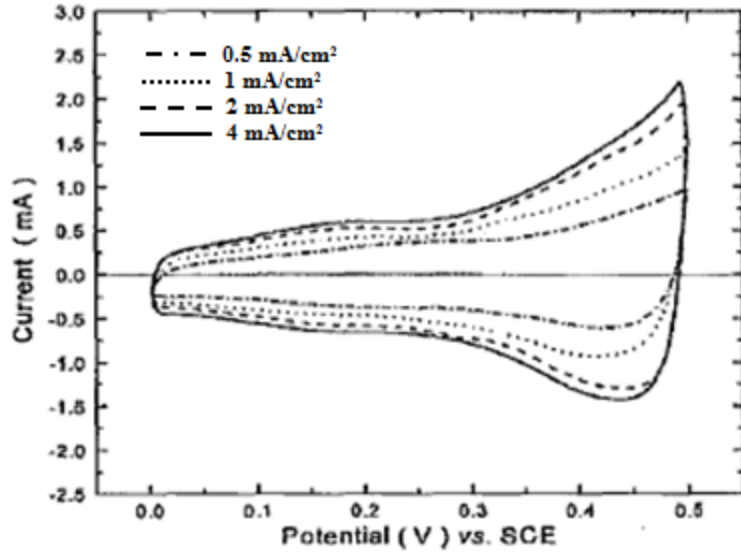
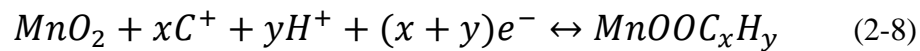


Figure 2-13 Cyclic voltammogram of nickel oxide [40].

2.5.2.1.4 Manganese oxide

Manganese oxides are attractive electrode materials for ES because they are inexpensive, possess excellent electrochemical properties and hence they are environmentally friendly compared to other transition metal oxides. Manganese oxide electrodes can be prepared by electrochemical deposition [42], precipitation method [43] or sol-gel route [44]. The charge storage mechanism of manganese dioxide can be expressed as [41]:



Surface adsorption of cations C^+ in the electrolyte and incorporation of proton forms the basis of storage mechanism. Manganese oxides exhibit ideal capacitive behaviour in cyclic voltammetry as shown in the Fig 2-14 [48].

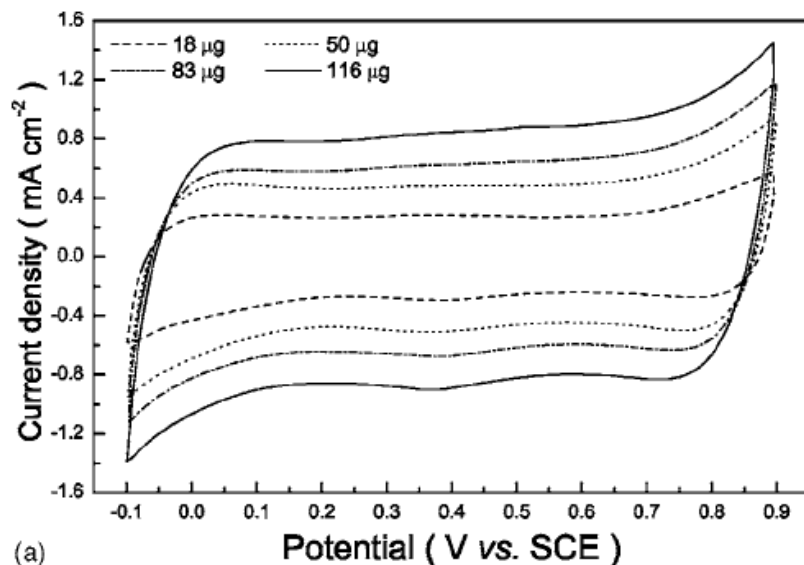


Figure 2-14 Cyclic voltammogram of manganese oxide [48].

2.5.2.2 Conducting polymers (CP)

Conducting polymers such as Polypyrrole (PPY), Polyaniline (PAn), Poly (3,4-ethylenedioxythiophene) (PEDOT), Polythiophene (PTh), and Poly (p-phenylene vinylene) (PPV) are considered as promising electrode materials for ES applications. The presence of overlapping π -conjugated polymer chains in the backbone increases the electrical conductivity. They possess high capacitance as the charging takes place over the whole bulk volume, low equivalent series resistance and higher conductivity than carbon-based electrode materials. They are relatively inexpensive and more environmentally friendly than transition metal oxide materials. The charging mechanism of conducting polymer is expressed in Figure 2-15 [45]. The electronic charge is injected into the polymer chain and the ionic charge transfer into the polymer matrix provides the charge neutrality [46]. There are two types of charging process, (i) p-doping and (ii) n-

doping. P-dopable polymers gained much attention because of their cycling stability compared to cycling degradation of n-dopable polymers [47]. The nature of dopant ions greatly influences the electrochemical and mechanical properties of the conducting polymer film. Other factors such as nature of monomers, electrolyte, pH of solution, the substrate, the deposition condition also plays significant role in determining the capacitance value of the conducting polymer film [48].

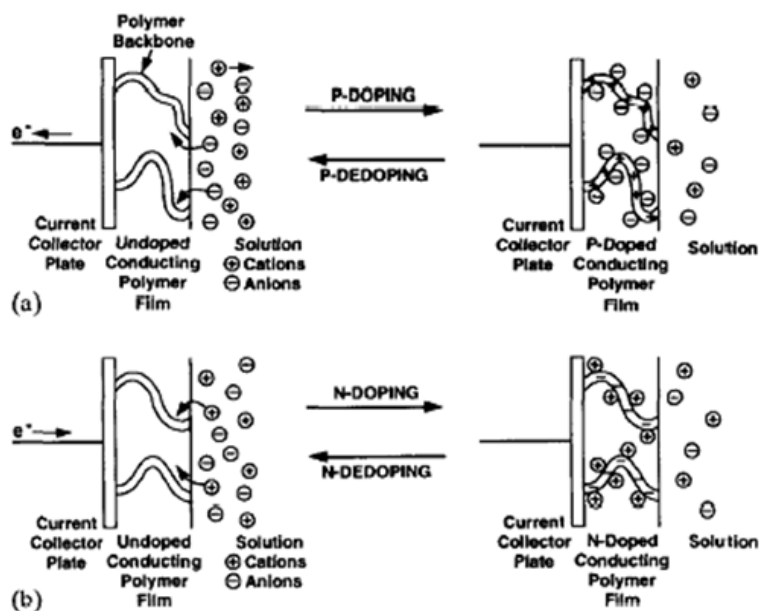


Figure 2-15 Charge storage mechanism of conducting polymer electrodes, (a) p-type and (b) n-type [45].

Besides various attractive properties, utilisation of conducting polymers as electrode materials was limited due to their lower cyclic stability compared to other

electrode materials. Due to the degradation caused by over-oxidation, the working potential range of the conducting polymer electrode is limited.

2.5.2.2.1 Properties of Conducting Polymers

Figure 2-16 shows the chemical structures of some of the common conducting polymers [93]. Based on the chemical structures, conducting polymers exist in different forms, which are aromatic, heterocyclic, benzenoid, or nonbenzenoid.

Electrical conductivity of organic polymer film at the electrode surface is due to the oxidation or reduction of these molecules. Three groups of polymers have been studied at present. They are (i) Polyacetylene (PA) which is a linear type polymer with simple structure, (ii) PPY and PTh which are polyheterocyclic polymers and (iii) Poly(p-phenylene) (PPP) and Poly (p-phenylene vinylene) (PPV) which are polyaromatic conducting polymers.

Conducting polymers are electrically conductive due to their extensively π -conjugated backbone. The degree of conductivity is influenced by the density and mobility of electrons. The nature of charge carriers such as solitons, polarons and bipolarons and the conjugation length also contributes the conductivity of conducting polymers [94]. Solitons, polarons and bipolarons are considered to be the main source of the charge carriers in conjugated polymers. However, electronic conduction mechanisms and the charge carriers generation are still under research.

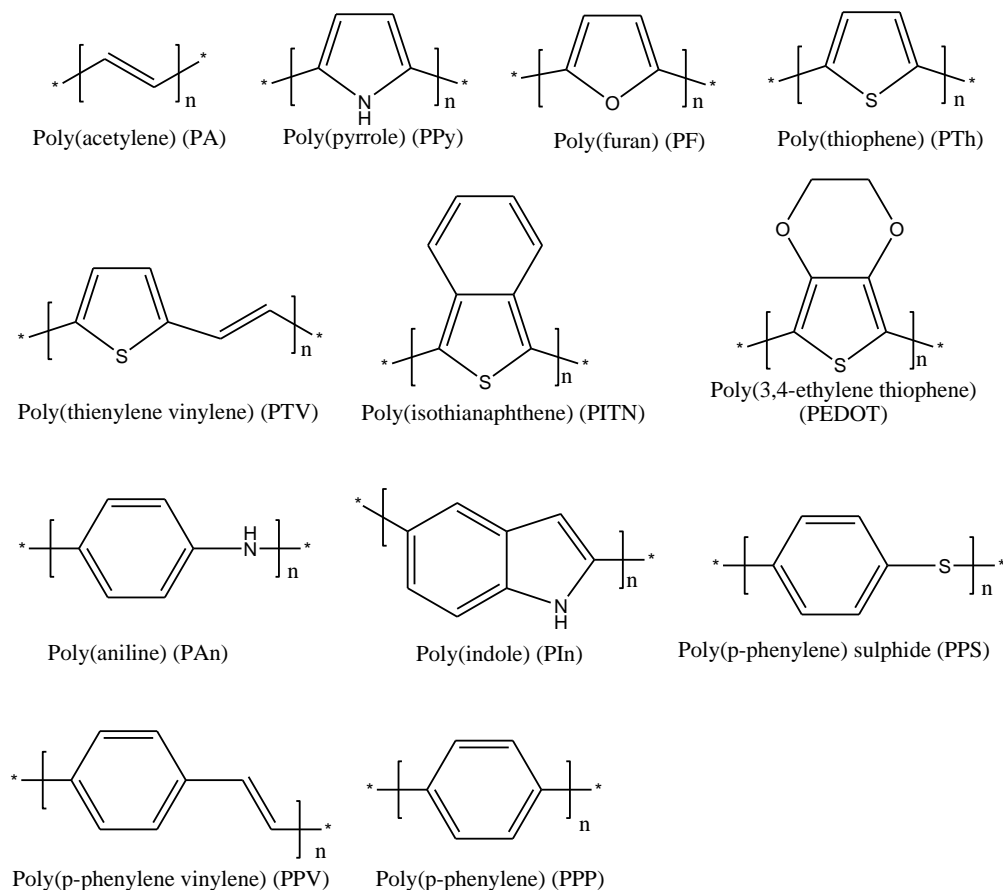


Figure 2-16 Chemical structure of common conducting polymers [93].

Based on quantum chemical theory and polymer science, various theoretical models have been proposed [93, 96-98]. The movement of charge carriers between localized sites or between solitons, polaron or bipolaron states are considered as the main mechanism. Conductivity is due to the charge transfer along the chain or between the different conjugated segments (domains) in the same chain. The electron hopping between different chains also results in the conductivity of the polymer. It was stated that the structural defects in the polymer backbone causes alternating change in single and double bonds. The degeneracy in PA or non-degeneracy in PPy and other conducting polymers of the ground state attributes to the structural defects. The possible structure of

PPy in non-degenerate configuration ((a) aromatic and (b) quinoid) and charge carrier defects ((c) polaron and (d) bipolaron), as shown in Figure 2-17 [96].

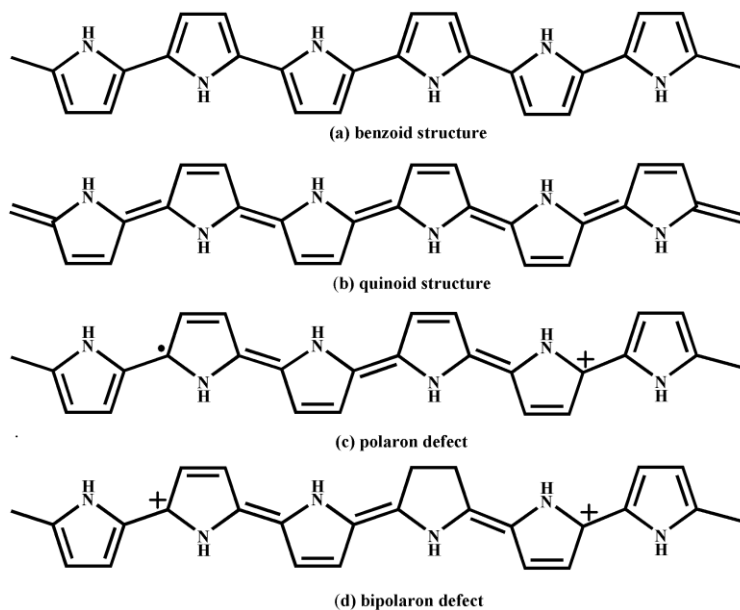


Figure 2-17 Non-degenerate ground state configurations and charge carrier defects of PPy [98].

The conjugated polymers in their undoped, pristine state are semiconductors or insulators. Undoped conjugated polymers, such as, polyacetylenes have a low electrical conductivity. But heavily iodine-doped polyacetylene exhibit a high conductivity value [99]. The conductivity of doped polymer depends on the nature of dopants or oxidants as well the doping temperature and the doping procedure [99-101].

Generally, there are two distinct types of stability of conducting polymers, (i) extrinsic stability and (ii) intrinsic stability. Extrinsic stability is related to vulnerability to external environmental agents such as oxygen, water which can attack the charged sites of polymers by the nature of nucleophilicity and electrophilicity. In ambient atmosphere, for

example, polyheterocyclic polymers, such as PPY and PTh exhibit much higher stability than does PA when exposed to the oxygen while PTh is more sensitive to water than is PPY [102]. Intrinsic stability of CPs is thermodynamic in origin. The degradation of CPs is likely due to the irreversible chemical reaction with main chain dopants or counter ions, leading to a break of conjugation and the loss of conductivity. The nature of dopants or counter-ions with respect to different polymers is the key factor affecting the conduction stability [103], under systematically controlled environmental and thermal conditions. The conduction stability of PPY was found to be significantly better than that of the poly(3-alkylthiophenes). PPY doped with arylsulfonates were found to exhibit excellent stability in inert atmospheres but were slightly less stable in the presence of dry or humid air. PPY samples doped with the tosylate anion were found to be the most stable, while PPY doped with longer side chain substituted benzenesulfonates exhibited poorer stability.

The conjugated polymer backbone in the doped form attributes to the electrical conductivity of polymers. But the resulting conducting polymers are insoluble, infusible and intractable. Processing of conducting polymers are difficult. Processing problems can be solved by modifying the structure of the polymer by attaching long flexible side groups to some separated monomers along the conjugated back bone. An example is copolymer poly(3-octylthiophene-co-3-methylthiophene) (POTMT) [104]. Another approach is to deposit the polymer in desired shape and form. For example, PAN/poly (sulfonated styrene) (PSS) nanofiber composites were prepared by the interfacial method [105]. PANI nanofibers in the presence of sulfonated polystyrene allows for the growth of PANI 2-D

nanostructures embedded in the polymerized sulfonated host. Some alignment of the aniline monomer onto the anionic dopant is suggested to be involved in the growth mechanism.

The reversible redox reaction which switches between an insulating state and conductive state is the unique electroactive behaviour of conducting polymer films. The process involves electron transitions and mass transport of ions and solvents unlike other redox system. For example, the oxidation of pyrrole yields a charged polymer film with incorporated anions; the pyrrole units are positively charged and compensated by incorporated anions. When negative potential is applied, the anions are expelled and the film obtains electrons to reduce to its neutral state. Conversely, when positive potential is applied, the anions are inserted into the film and the pyrrole units lose electrons and transform to an oxidized state.

The dopant anion of small size can be exchanged with electrolyte anions during potential sweeping. During the reduction of the polymer, the immobilized polymeric dopants or large surfactant anions are not released. Therefore, the charge balance in the film is maintained. The electrolyte cations are incorporated into the PPy matrix. Hence, the cation transport is involved in the electrochemistry of PPy/polyanions film [107,108].

2.5.2.3 Composite materials

The objective of the development of composite material electrodes is to combine the attractive properties of the individual materials into a single electrode. Composite

materials comprise two or more materials that are discussed earlier. When high surface area carbon based materials combined with redox pseudocapacitive materials, the overall capacitance is significantly larger because of the combination of double layer capacitance and pseudocapacitance.

2.5.2.3.1 CNT-CP Composites

In the study of Sahoo [49] et al., CNT and polymer composites showed high mechanical strength and reduced degradation of the film after repeated cycles. The CNT-PPY composite exhibited improved electrochemical performance. The electrochemical capacitance of CNT-PPY composite was 6 times higher than that of pure PPY in organic electrolyte [50]. The cyclic voltammograms (Figure 2-18) showed improved capacitive behaviour of CNT-PPY composites compared to the pure PPY. It was also reported that CNT reinforcement of PPY reduced the swelling and shrinkage of PPY during charge-discharge process.

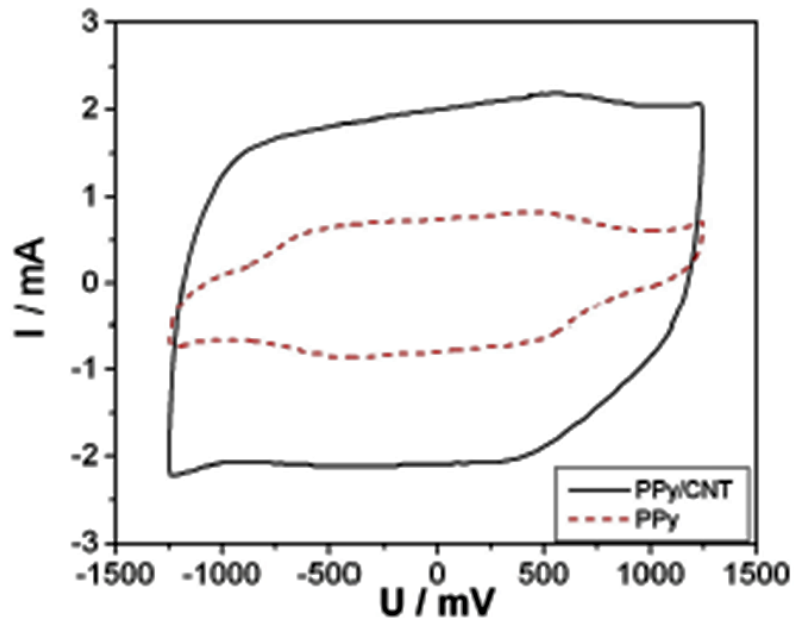


Figure 2-18 Cyclic voltammograms of pure PPY and PPY-CNT composite at scan rate of 20 mV/s [50].

2.5.2.3.2 Metal oxide – CP composites

In the study of Zhang [51] et al., synthesis of PPY-MnO₂ composite was carried out by delamination/reassembling process. The results showed that PPY-MnO₂ composite showed much higher conductivity (about 4-5 orders of magnitude) than that of pristine manganese oxide at room temperature. The improved capacitive behaviour of the composite can be clearly seen from the cyclic voltammograms presented in the Figure 2-19. The combined effect of high conductivity of composite and high specific capacitance of PPY resulted in the improved specific capacitance of PPY-MnO₂ composite than that of pristine manganese oxide.

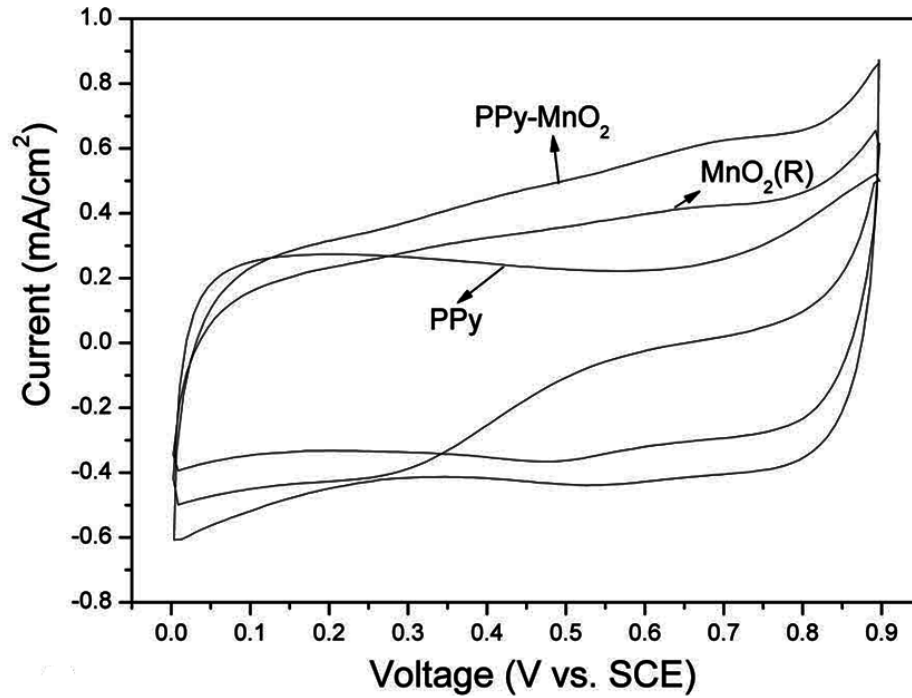


Figure 2-19 Cyclic voltammograms of PPY, MnO₂ and PPY-MnO₂ at a scan rate of 5 mV/s [51].

2.6 Electrolytes

The properties of electrolytes play a vital role in the electrochemical behaviour of ES. The power density of ES is controlled by the resistance of the electrolyte. The energy density of ES is governed by the operating voltage which is restricted by the breakdown potential of the electrolyte. There are three different types of electrolytes used in ES: (i) aqueous, (ii) organic and (iii) ionic.

Table 2-2 Comparison of aqueous electrolyte and organic electrolyte [56].

| Aqueous Electrolytes | Organic Electrolytes |
|--|---|
| Unit cell voltage is limited to typically 1V which reduces the energy density. | Unit cell voltage is above 2V which results in comparatively high energy density. |
| Low specific resistance and hence high power density can be achieved. | Specific resistance higher than that of aqueous electrolyte by a factor of at least 20 resulting in low power density. |
| Purification and drying process are less stringent comparatively. | Requires very stringent purification and drying process during production otherwise formation of H ₂ and O ₂ occurs on charging and subsequent recombination reactions leads to self-discharge. |
| Less expensive. | Relatively more expensive. |

2.6.1 Aqueous Electrolytes

The most commonly used aqueous electrolytes for ES are acid and alkaline electrolytes. High conductivity and mechanism of proton transport of acid and alkaline electrolytes are the attractive properties for application of ES. In aqueous electrolyte, the proton with high mobility and small size chemisorbs to a single oxide ion. High

concentration of electrolytes enables to reduce the ESR and improve the conductivity. Concentrated sulphuric acid is used as electrolytes for RuO₂ electrodes which avoids electrolyte depletion problems during charging [34,52]. The use of concentrated acids results in harmful effects to environment and increases the corrosiveness of the electrode. Also the unit cell voltage is limited to 1V which results in low energy density. Mild potassium chloride aqueous electrolyte is also used for MnO₂ electrodes for ES [53]. Sodium chloride is another most widely used aqueous electrolyte for ES [54,55].

2.6.2 Organic Electrolytes

Organic electrolytes are mostly based on acetonitrile or propylene carbonates which allow operating ES in the voltage range of 2 – 2.5V. Therefore, higher energy density can be achieved than that of when aqueous electrolyte is used. The solubility of salts in organic solvents is relatively low. Organic electrolytes possess higher resistivity than concentrated aqueous electrolytes. Because of large size of the organic molecules, the requirement of the pore size of the electrode is greater [12]. Hence the power density of ES is greatly reduced. Tetraethyl ammonium salts have been considered as suitable electrolyte because of their good solubility and conductivity in organic solvents [56].

2.6.3 Ionic electrolytes

Ionic electrolytes are composed of bulky organic cations and different anions. They enable to increase the voltage range of ES. Ionic liquid has no solvent molecules like other electrolytes which dissolves salts in molecular solvents. At room temperature, they are generally liquid with high thermal and electrochemical stability. They possess negligible vapour pressure.

ES with ionic electrolytes exhibits high energy and power density since the operating voltage is increased to 3.4V [56]. The commercial usage of ionic electrolytes in ES is limited because of high cost.

2.7 Fabrication of CP Electrodes

Depending on the type of doping (n-type or p-type), CPs are classified as cationic or anionic salts of highly conjugated polymers. Cationic polymers are most commonly used for ES applications. They can be synthesised by simultaneous oxidation and polymerization from their respective monomers. Chemical polymerization and electrochemical polymerization are most commonly used methods for synthesis of CPs [57,58].

2.7.1 Chemical Polymerization

Chemical synthesis is the appropriate method for mass production of CPs. In this method, CPs is obtained in the form of powdery bulk materials in fast and simple process. Chemical oxidants are used for synthesis of PPY. The properties of final product are

determined by various factors such as nature of oxidants, concentration ratio of oxidant to monomer, temperature of reaction, nature and concentration of solution components. Chemical polymerization of PPY is carried out using various oxidants such as cerium(IV) sulphate [60]. High conducting PPY films are synthesised when pyrrole reacted with copper(II) perchlorate in acetonitrile solution [61]. Iron(III) chloride is most commonly used to synthesis PPY in its oxidized form. In this method, oxidization of pyrrole takes place resulting in the formation of cation radicals. The formed cation radicals react with monomers forming dimers. This chain continues and ends with the formation of final product PPY polymer.

2.7.2 Electrochemical Polymerization

Diaz's mechanism [62] is most commonly used to explain electropolymerization. The mechanism of electrochemical polymerization is similar to that of chemical synthesis. The chemical oxidants are not used in electrochemical polymerization. The reaction mechanism is described as electron transfer, which is followed by successive chemical reactions. The mechanism is explained in Figure 2-20.

Electropolymerization does not give neutral non-conducting PPY but its oxidized (doped) form. Anion and electron transport are essential for PPY film formation. In the Figure 2-20, A^- is the counter anion incorporated during polymerization to maintain the charge balance in the polymer backbone. Depending on the type and the charge of the dopant ion, the value n was determined to be 2.2-2.4. The doping level is usually between 0.2-0.3 for PPY, corresponding to one charge compensated by 3-4 pyrrole units to

achieve electro neutrality [63]. Obtained PPY film consists of 65% polymer and 35% anion by weight.

Electrochemical polymerization is a facile way for synthesis of polymer films. Properties of the films are controlled by polymerization parameters such as potential, current density, electrolyte, concentration of monomer, nature of substrate, solvent, etc.

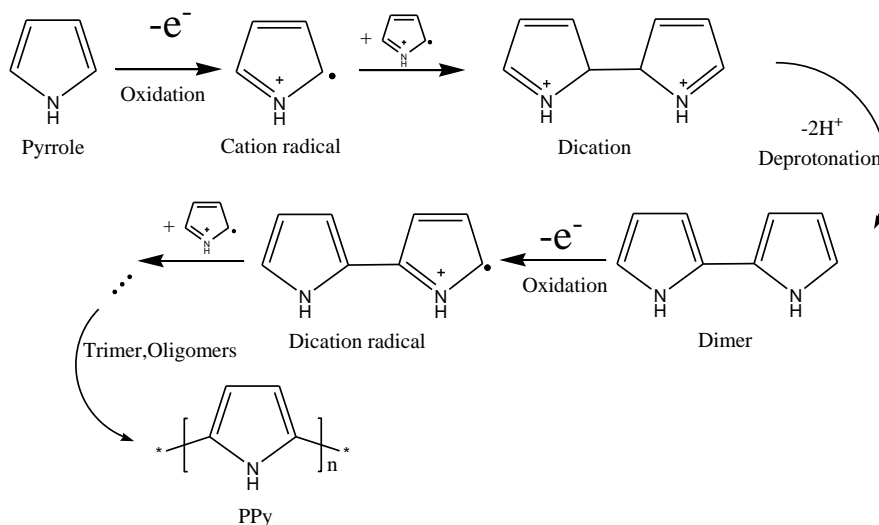


Figure 2-20 Mechanism of electropolymerization of PPY [62].

Various advantages and disadvantages of chemical and electrochemical polymerization are expressed in Table 2-3 [59].

Table 2-3 Comparison of chemical and electrochemical polymerization [59].

| Polymerization approach | Advantages | Disadvantages |
|---------------------------------------|---|---|
| Chemical polymerization | <ul style="list-style-type: none"> • Large-scale production possible. • Post-covalent modification of bulk CP possible. • More options to modify CP backbone covalently. | <ul style="list-style-type: none"> • Synthesis more complicated. • Can not make thin films. |
| Electrochemical polymerization | <ul style="list-style-type: none"> • Thin film synthesis possible. • Ease and better control of synthesis. • Entrapment of molecules in CP. • Simultaneous polymerization and film formation. | <ul style="list-style-type: none"> • Post-covalent modification of bulk of CP is difficult. |

2.7.3 Effect of solvent

Solvents have significant influence on the morphology and conductivity of the film. They must be chemically inert to monomers and electrodes. Nucleophilic properties of the solvent determine the conductivity which was represented by donor number (DN). The conductivity of PPY films is inversely proportional to the DN value of the solvents [65]. Therefore, aprotic solvents which have poor nucleophilic character, such as acetonitrile, are used in common. Dimethyl sulfoxide which is a nucleophilic solvent, prevents the formation of polymer. Although PPY can be synthesised from organic and aqueous solutions, the conductivity is found to be higher in aqueous solutions than in

acetonitrile solution [66]. PPY is one of the few heterocycles that can be prepared in aqueous solutions. Compared to other heterocyclic monomers, the oxidation of pyrrole can be achieved at relatively low potential (0.8V vs. SCE), which is also lower than the decomposition potential of water.

2.7.4 Effect of dopant ions

The inorganic and organic anions incorporated into the polymer affect the redox behaviour, morphology and electric conductivity of the PPY film during synthesis. The behaviours of different anions like Cl^- , Br^- , NO_3^- , ClO_4^- indicated that the size and mobility of the anion greatly affects the redox activity of PPY film [67]. The effect of dopants on the kinetic formation and the electrochemical behaviour of PPY film have been studied, the results showed that the dopants had a strong influence on the electropolymerization process of polymer films [68].

2.7.5 Effect of pH

The pH has influence on reactivity, stability, conductivity and electrochemical activity of PPY. At low pH, electropolymerization is greatly favoured but the films showed low conductivity [69]. The adhesive strength of PPY film on steel substrate was poor at high pH, the film exhibited high adhesion when the pH of the solutions was below 4.1 [70].

2.7.6 Effect of temperature

Processing temperature plays a role in the quality and morphology as well as conductivity and redox activity of PPY films. The effect of temperature on electropolymerization of pyrrole in oxalic acid solution on a mild steel substrate has been studied [71]. In acidic medium, lower temperatures favoured the overall process. At higher temperature and lower current densities, oscillations in electrode potential were observed due to the occurrence of iron dissolution before oxidation of pyrrole. In alkaline medium, higher temperatures favoured the process and better quality films were obtained.

In the study of Li [72], PPY thin films have been synthesised on glass by several methods like cyclic voltammetry, potentiostatic and galvanostatic deposition methods. In a cyclic voltammetry experiments, the higher the redox peaks, the activity of electrochemical reaction is higher. The results showed that galvanostatic deposition of PPY film could produce higher electrochemical reactivity than in the cyclic voltammetry and potentiostatic deposition methods. Hence, the constant current method is widely adopted in the preparation of PPY. Optimization of various parameters is difficult due to the complexity of the electrochemical polymerization process for the preparation of PPY film. Several research works have been done focusing on the optimization of process parameters.

3 Objectives

The objective of this work is to develop advanced electrode materials for ES based on following considerations.

- **Materials:** Synthesis of novel electrode materials using nanostructured conducting polymer PPY for ES.
- **Processing techniques:** The development of anodic electropolymerization process for fabricating conducting polymer PPY coatings on stainless steel substrates using novel additives.
- **Characterisation:** Investigate the kinetics of deposition and deposition mechanism. Optimize the bath composition and deposition parameters. Investigate the microstructure and electrochemical properties of PPY films such as capacitance, impedance, cyclic stability and corrosion protection.
- **Design factors:** Development of advanced electrode material using novel plating additives.

4 Approach and methodology

4.1 Approach

Anodic polymerization has been adopted to deposit PPY films on stainless steel substrates. Deposition was carried out at galvanostatic conditions from aqueous solution containing pyrrole and selected additives.

4.2 Methodology

4.2.1 Dissolution of substrate

The major problem of electropolymerization of PPY on active metal substrate is the dissolution of metal substrate, which takes place before polymerization. Since the oxidation potential of active metals such as stainless steel is much lower than the polymerization potential of pyrrole, the dissolution of metal prevents the oxidation of pyrrole and hence restricts the PPY film formation on metal substrate. S. Wencheng [64] et al., reported that the PPY films were successfully deposited on steel substrate from aqueous oxalate solution. During the process, the oxalate ions form a passive layer on steel. On further oxidation, the decomposition of passive layer takes place followed by the electropolymerization of pyrrole when the polymerization potential was reached. But the passivation occurs after a long induction time as shown in the chronopotentiometry curve in Figure 4-1 [64]. Resulting film showed poor adhesion strength at high pH.

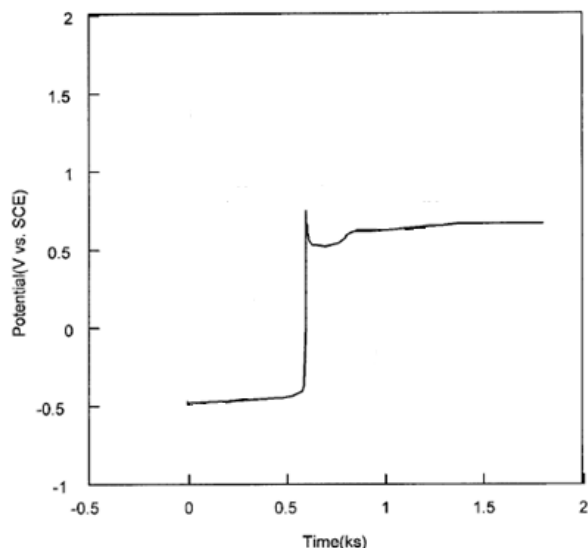


Figure 4-1 Chronopotentiometry curve for formation of PPY coating on steel in the solution of pH 1.4 at current density of 0.56 mA cm^{-2} [64].

4.2.2 Role of anionic additives

Considering the complications involved in electropolymerization of PPY on active substrates, new anionic additives are implemented in the process. The additives are expected to perform anionic doping of CP during electropolymerization, reduce the dissolution of metal substrate due to complexation with metal ions, act as electron transfer mediator and improve the adhesion of the polymer film.

The approach is based on recent fundamental studies of the chemical mechanism of strong mussel adhesion to inorganic surfaces in water. The adhesion mechanism of mussel to metal and metal oxide surfaces in underwater environment was studied in the literature [73]. It was reported that the adhesion is due to the strong bond formation of

dopamine with metal and metal oxides because of the formation of interfacial chemisorption complexes. This bio-inspired approach created interest in the study of adhesion mechanism of organic compounds on oxide surfaces [74-79]. It was also reported that the deprotonation of OH groups of catechol and their ability to form mononuclear or binuclear chelates is responsible for the adsorption mechanism [80]. The study of K. Wu [81] et al., showed that the presence of adjacent OH group bonded to aromatic ring in dopamine and gallic acid enhances the adsorption of molecules on the oxide particles. Chromotropic acid (CHR) showed strong adsorption towards oxide particles [82]. Figure 4-2 shows the structure of CHR and gallic acid and possible complexation on metal oxides where M denotes metal atom on the surface [81,82].

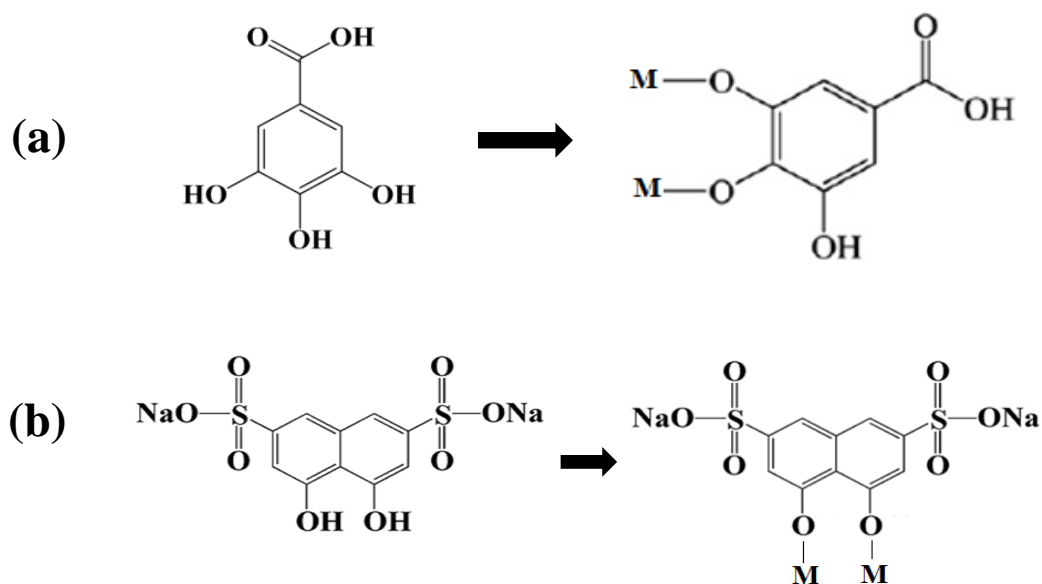


Figure 4-2 Chemical structure and possible complexation on metal oxides of (a) gallic acid and (b) CHR [81,82].

Hence CHR and gallic acid are selected for the electropolymerization of PPY on stainless steel substrate. Conjugate bonds provided high conductance and electron transfer mediation.

5 Experimental Procedures

5.1 Starting Materials

Chromotropic acid (CHR) and Gallic acid were purchased from Sigma Aldrich. Pyrrole (98⁺%) was purchased from Alfa Aesar. 304 annealed stainless steel foil of dimension 50 x 30 x 0.05 mm was purchased from McMaster Carr Supply Company.

5.2 Experiment Set-up

Electrodeposition was carried out at constant current provided by EPS 2A200, Amersham Biosciences. Stainless steel substrate in which the deposition of PPY has to be done is used as anode and platinum is used as cathode. Electrochemical testing such as cyclic voltammetry, chronopotentiometry, electrochemical impedance spectroscopy and Tafel testing were performed using potentiostat (PARSTAT 2273, Princeton Applied Research).

5.3 Electropolymerization and Electrodeposition of PPY

Electropolymerization, doping and film formation are simultaneously carried out in electrodeposition process. Pyrrole of concentration 50 – 150 mM was dissolved in 275 mL of deionized water. CHR or Gallic acid of concentration 5 – 50 mM was further added to the pyrrole solution. The aqueous solution was stirred during appropriate time depending upon the concentration of mixture. Electrodeposition was performed from the solution containing the mixture. Stainless steel substrates of dimension 2.5 cm x 5 cm

were used as anode and thin platinum plates of same dimension were used as cathodes. Platinum plates were placed on either side of the stainless steel substrate separated at a distance of 15 mm. Electrodeposition was performed at a constant current of 0.7 mA cm^{-2} . The time of deposition was varied from 1 to 15 minutes. After deposition, the stainless steel substrate with PPY film deposited is allowed to dry at room temperature. The schematic diagram of electrodeposition process is shown in the Figure 5-1.

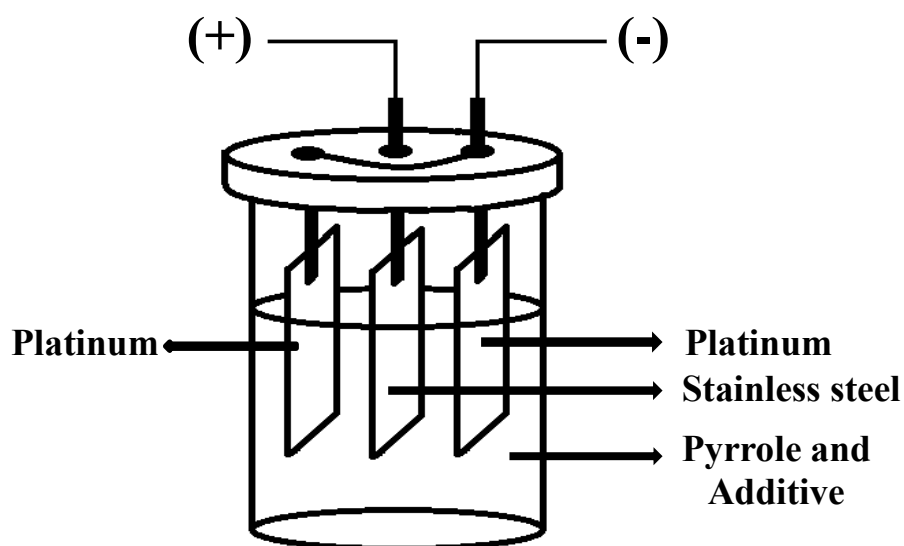


Figure 5-1 Schematic representation of experimental set-up in electrodeposition.

5.4 PPY film Characterization

5.4.1 Electrochemical characterization

PPY film deposited by electrodeposition was subjected to different electrochemical testings performed using potentiostat (PARSTAT 2273, Princeton Applied Research). The potentiostat was connected to a computer and controlled by PowerSuite electrochemical software. The testings were conducted in a standard three electrode electrochemical cell. The area of 1 cm² of the working electrode was exposed to the electrolyte. Platinum gauze was used as counter electrode. Standard calomel electrode (SCE in saturated KCl solution) was used as a reference electrode. Na₂SO₄ aqueous solution of concentration 0.5 M was used as electrolyte and it was deaerated by purging purified nitrogen gas before and during electrochemical measurements.

Cyclic voltammetry (CV) was performed for PPY films at different scan rates from 2 – 100 mV s⁻¹ in the voltage range of -0.5 to 0.4 V vs SCE. From the obtained voltammograms, the charge accumulated (Q) can be calculated by integrating the half of the area under the CV curve. Hence specific capacitance (SC) can be calculated by the equation:

$$C = \frac{Q}{m\Delta V} \quad (5-1)$$

where m is the mass of the film and ΔV is the potential window.

Electrochemical impedance spectroscopy (EIS) was performed in the similar electrochemical cell as CV. The a.c. impedance of the films was investigated in the frequency range of 0.05 Hz to 100 kHz at an applied a.c. signal of 5 mV r.m.s. Equivalent circuits for impedance spectra of PPY films were obtained using ZSIMPWIN software.

Chronopotentiometry tests were performed at a constant current density of 1 mA cm⁻². The potential vs time curve obtained was used to compare the electropolymerization potential of different PPY films.

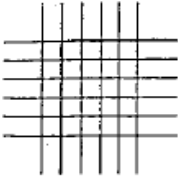
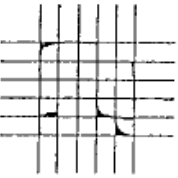
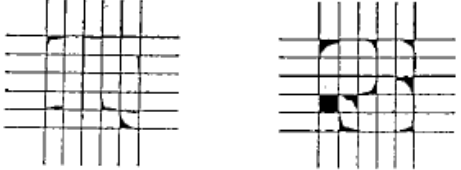
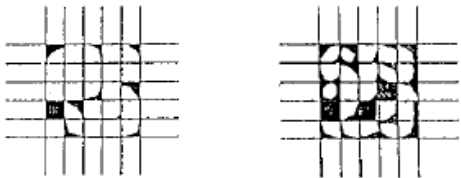
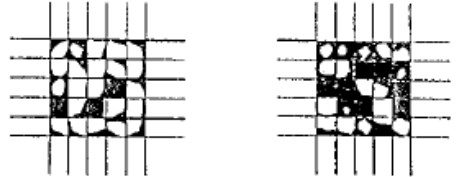
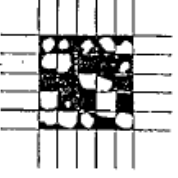
5.4.2 Morphology Characterization

The microstructure and morphology of electrodeposited films were studied using a JEOL JSM-700F Scanning Electron Microscope (SEM). Surface of PPY films were observed at high magnification (up to 30000X). Deposits were platinum - coated by sputtering before observation.

5.4.3 Adhesion Test

PPY films electrodeposited on stainless steel are subjected to Tape test. Parallel cuts were made horizontally and vertically on flat surface of the PPY coated substrate. Tape is placed on the grid area and pressure is applied over the surface. Tape is removed from the substrate and compared with ASTM D3359 standards as shown in the Table 5-1.

Table 5-1 Classification of Adhesion Test Results

| CLASSIFICATION | PERCENT AREA REMOVED | SURFACE OF CROSS-CUT AREA FROM WHICH FLAKING HAS OCCURRED FOR SIX PARALLEL CUTS AND ADHESION RANGE BY PERCENT |
|----------------|----------------------|---|
| 5B | 0% None |  |
| 4B | Less than 5% |  |
| 3B | 5 - 15% |  |
| 2B | 15 - 35% |  |
| 1B | 35 - 65% |  |
| 0B | Greater than 65% |  |

6 Results and Discussions

6.1 Electropolymerization of PPY doped with CHR

6.1.1 Cyclic Voltammogram Electropolymerization of PPY

The cyclic voltammogram of the sweeps recorded during the electrodeposition of PPY film on the stainless steel electrode from aqueous solution containing 5 mM CHR and 50 mM pyrrole is shown in Figure 6-1.

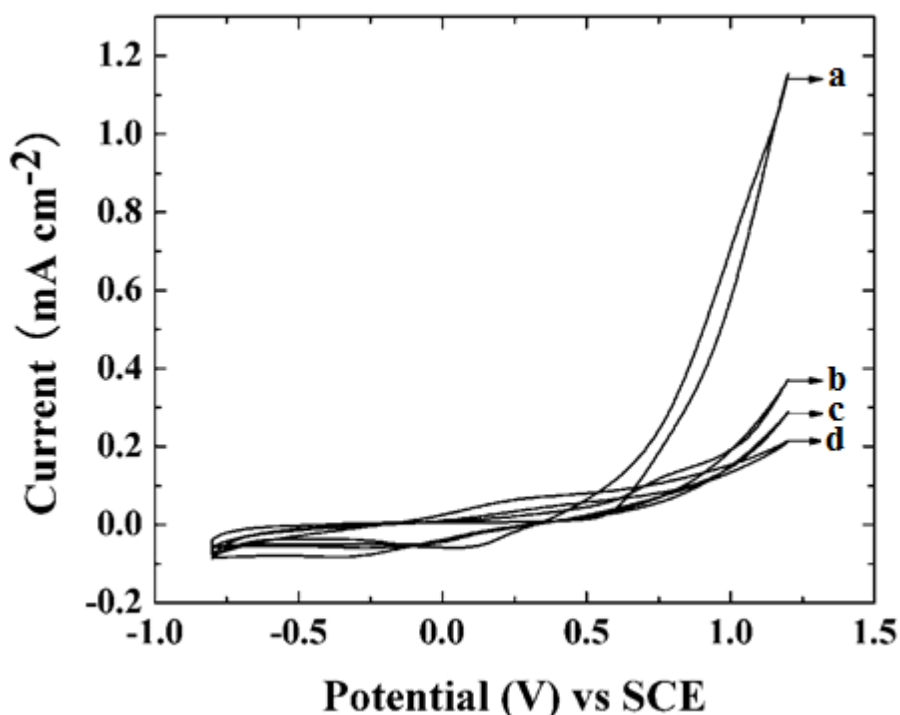


Figure 6-1 Cyclic voltammograms at (a) 1st cycle, (b) 2nd cycle, (c) 3rd cycle and (d) 10th cycle for stainless steel electrode in 50 mM pyrrole solution containing 5 mM CHR at a scan rate of 20 mV s⁻¹.

The first positive cycle was characterized by a sharp increase in the anodic current above ~ 0.6 V. The increase in anodic current was attributed to electropolymerization of PPY. The black films were formed at the stainless steel electrode at potentials above 0.6 V. The deposit was formed as a result to the chain reaction of pyrrole units with cation radicals, and the polymerization on the metal surface. However, the current corresponding to the anodic electropolymerization decreased gradually with the number of scans. It should be noted that the conductivity of PPY is lower than the conductivity of the stainless steel substrates. Therefore, film growth during cycling resulted in the decrease in current with increasing cycle number.

6.1.2 Galvanostatic Electropolymerization of PPY

The PPY films are deposited on stainless steel substrates at a constant current density of 1 mA cm^{-2} from the solution containing 50 mM pyrrole and 5 mM CHR. In order to understand the influence of OH group of CHR, the deposition was also performed in the solution containing 50 mM pyrrole and 5 mM of 2,6-naphthalenedisulfonic acid disodium salt (NSA) under the same conditions. Chemical structures of CHR and NSA are compared in Figure 6-2 a, b.

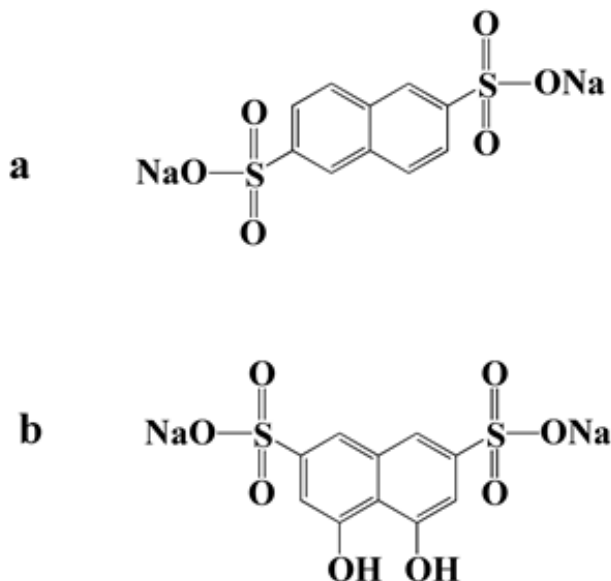


Figure 6-2 The chemical structure of (a) 2,6-Naphthalenedisulfonic acid, disodium salt (NSA) and (b) Chromotropic acid disodium salt dihydrate (CHR).

Electropolymerization was carried out within the deposition time of 10 minutes for both the cases. Uniform and adherent films were obtained. The results obtained are shown in Figure 6-3. The chronopotentiometry curves indicate that there is no induction time for electropolymerization of PPY on the stainless steel substrates. In contrast, the deposition of PPY on stainless steel from the solutions containing oxalic acid revealed the presence of an induction period, related to the dissolution of iron and formation of an iron oxalate layer. Both CHR and NSA facilitated a two-stage nucleation and growth process during the electropolymerization of PPY as an electron transfer mediator. Figure 6-3 indicates that at the beginning of the electrodeposition process, the potential difference between the working and reference electrode increased and then decreased to a steady value. It was observed that the polymerization potential of PPY in the presence of CHR

was ~ 0.4 V lower than that for NSA. The oxidation of pyrrole units to radical cations is facilitated in the presence of additives. This can be attributed to the conductive passive layer formed due to the complexation of additives with iron on the substrate surface. The comparison of the chemical structures of CHR and NSA in Figure 6-2 and the experimental results shown in Figure 6-3 indicated that OH groups of CHR were beneficial for the application of this material as an additive for PPY electropolymerization on stainless steel substrates. As discussed in the methodology, the adsorption mechanism was attributed to the deprotonation of OH groups and surface complexation of metal ions on the material surface. The adsorption of CHR was favoured by the presence of the two OH groups.

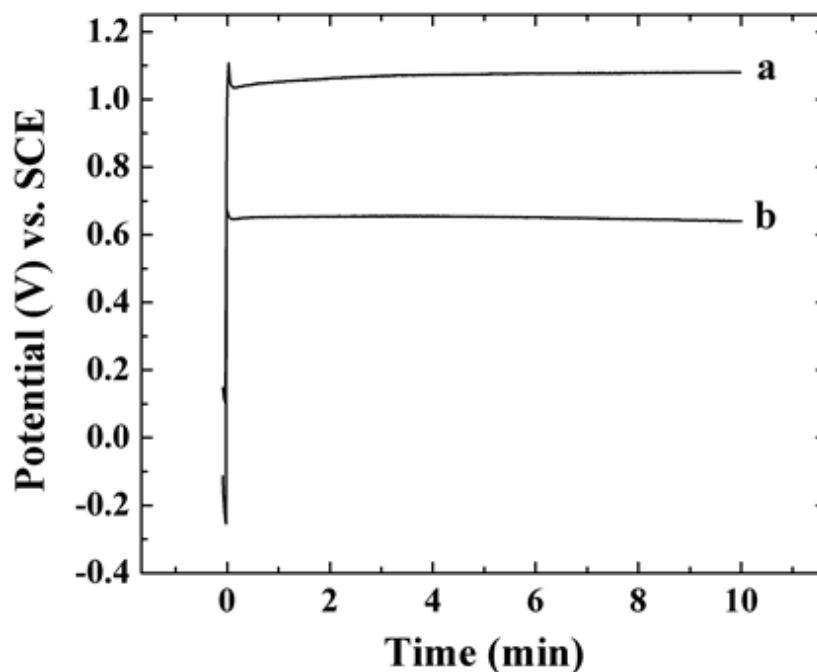


Figure 6-3 Potential versus time curves for galvanostatic deposition of PPY at a current density of 1mA cm^{-2} from 50 mM pyrrole solution in presence of (a) 5 mM NSA and (b) 5 mM CHR.

The reduced polymerization potential is beneficial for suppressing the substrate dissolution. It was suggested that the adsorbed CHR provided wiring between the substrate and the growing PPY film, promoted charge transfer during electropolymerization, and reduced the deposition potential. Moreover, the anionic CHR was incorporated into the PPY to ensure the electrical neutrality of the film.

6.1.3 Characterizations of PPY Film

6.1.3.1 Deposit Mass and Morphology Characterization

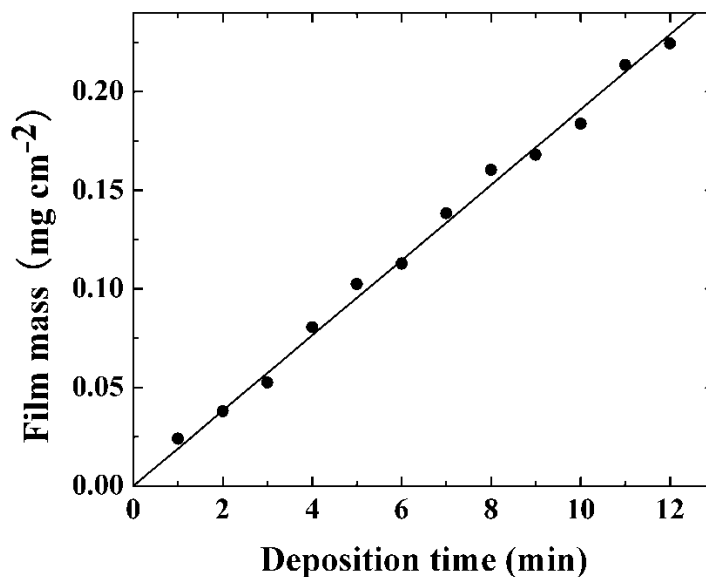


Figure 6-4 Film mass versus deposition time for films deposited from 50 mM pyrrole solution containing 5 mM CHR at a current density of 1 mA cm⁻².

Anodic polymerization was carried out on stainless steel substrate from solution containing 50 mM pyrrole and 5 mM CHR and strongly adherent PPY films were obtained. Almost linear dependences were obtained as shown in Figure 6-4. The film mass increased with increasing deposition time at a constant current density of 1 mA cm^{-2} condition. Therefore, the amount of the deposited materials can be controlled by the variation of deposition time at a constant current density and hence thickness of the films can be controlled.

Strongly adherent films on a stainless steel foil were obtained from pyrrole solutions containing CHR. The SEM surface images at low and high magnification are shown in Figure 6-5. At low magnification (Figure 6-5 a), it was observed that the film is smooth and crack free. At high magnification (Figure 6-5 b), finer particles of PPY were observed.

According to the nucleation and growth (NG) theory [84], it was suggested that the lower roughness surface can be attributed to the addition of CHR which can mediate the PPY film deposition by generating additional nucleation sites (progressive nucleation) and growing new polymer particles on the existing layer, resulting in a relatively smooth uniform surface structure.

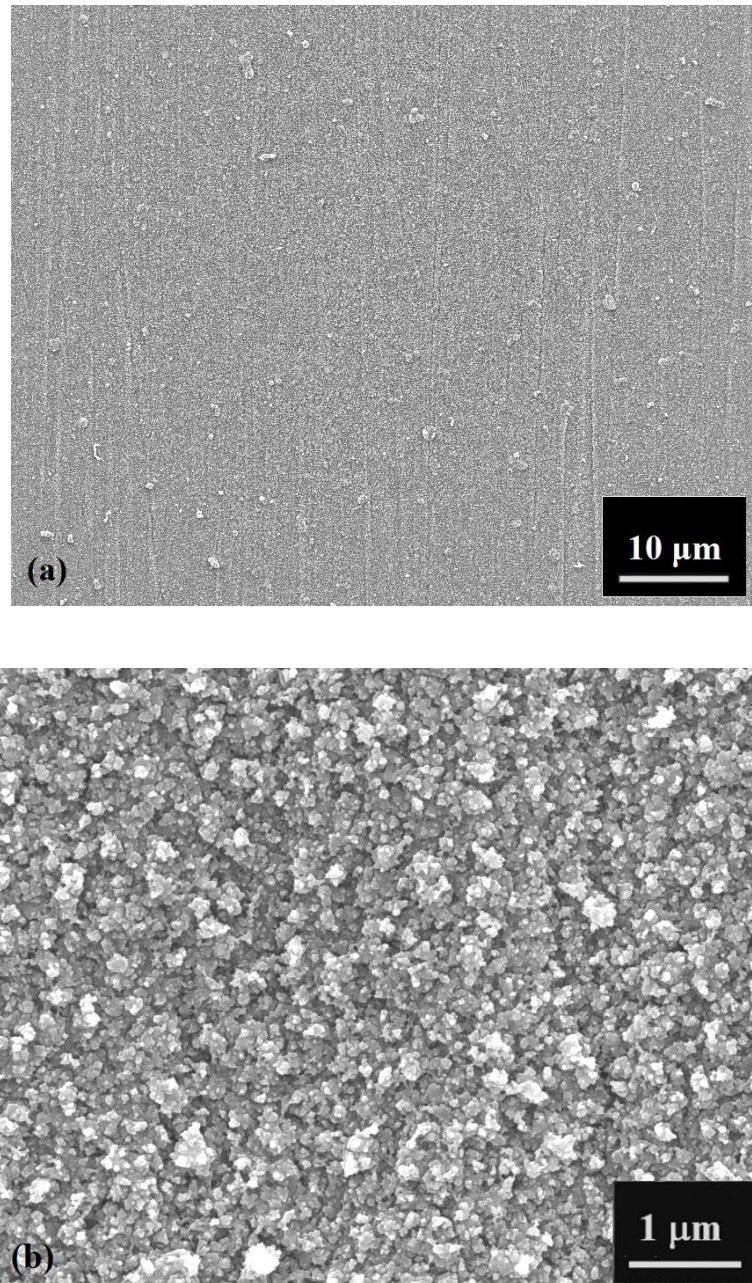
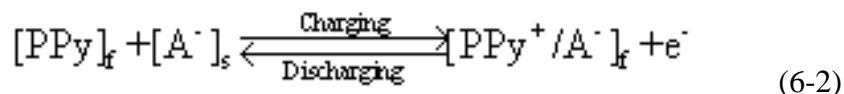


Figure 6-5 SEM images of surface of PPY film doped with CHR on stainless steel shown at a (a) low magnification and (b) high magnification.

6.1.3.2 Redox Reaction Properties

The electrochemical properties of the films prepared from pyrrole solution containing CHR were studied in 0.5 M Na₂SO₄ solutions using cyclic voltammograms (CV) as shown in Figure 6-6. At low scan rates, the films show good capacitive behaviour in the voltage window of 0.9 V between -0.5 - 0.4 V. The CVs show that PPY film exhibits improved capacitive behaviour in the negative potential window range. The area of CVs increased with increasing scan rate. A broad anodic peak at ~ -0.2 V and a cathodic peak at ~ -0.25 V were observed. It is proposed that the majority of CHR ions doped during PPY synthesis still exist in the inner layer of film due to its relatively large size, leading to poor mobility of CHR anions within the polymer matrix.

It is also suggested that strong charge-discharge behaviour is related to cation transport properties. The supporting electrolyte cations (in this case, ion Na⁺) readily diffuse in and out of the polymer during the redox process, in order to neutralize the immobilized charge of PPY film by the insertion of sodium cations (Na⁺) [85, 86]. The anodic and cathodic peak indicates release and insertion of Na⁺ during the positive and negative scan, respectively. The CVs show that the film exhibits both anion and cation-exchange properties. The redox reactions of film matrix can be expressed as follows:



Here, A⁻ is anions of electrolyte.

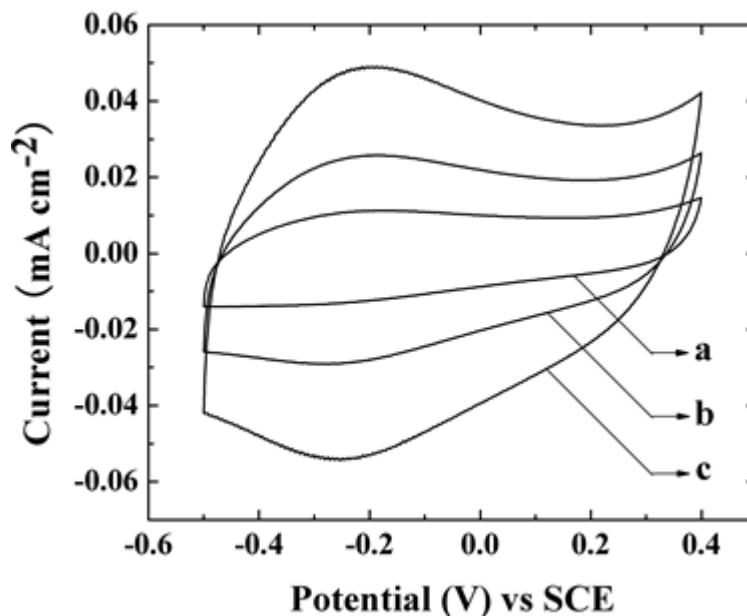


Figure 6-6 Cyclic voltammograms at scan rates of (a) 2, (b) 5 and (c) 10 mV s⁻¹ in 0.5 M Na₂SO₄ solution for 0.17 mg cm⁻² PPY film, prepared from the solution containing 100 mM pyrrole and 5 mM CHR.

6.1.3.3 Specific Capacitance (SC) of PPY film doped with CHR

6.1.3.3.1 Effect of concentration of CHR and Pyrrole on SC

To examine the relationship between SC and concentration of CHR and Pyrrole, PPY films were deposited at a constant current on stainless steel from the solution containing CHR whose concentration varied from 5 mM to 50 mM and Pyrrole whose concentration varied from 50 mM to 150 mM. The concentration range of CHR in solutions used for electropolymerization was limited by the solubility of this material in water. Figure 6-7 a, b, c, d and e shows CV of the PPY films prepared from solution with different concentration of CHR and Pyrrole.

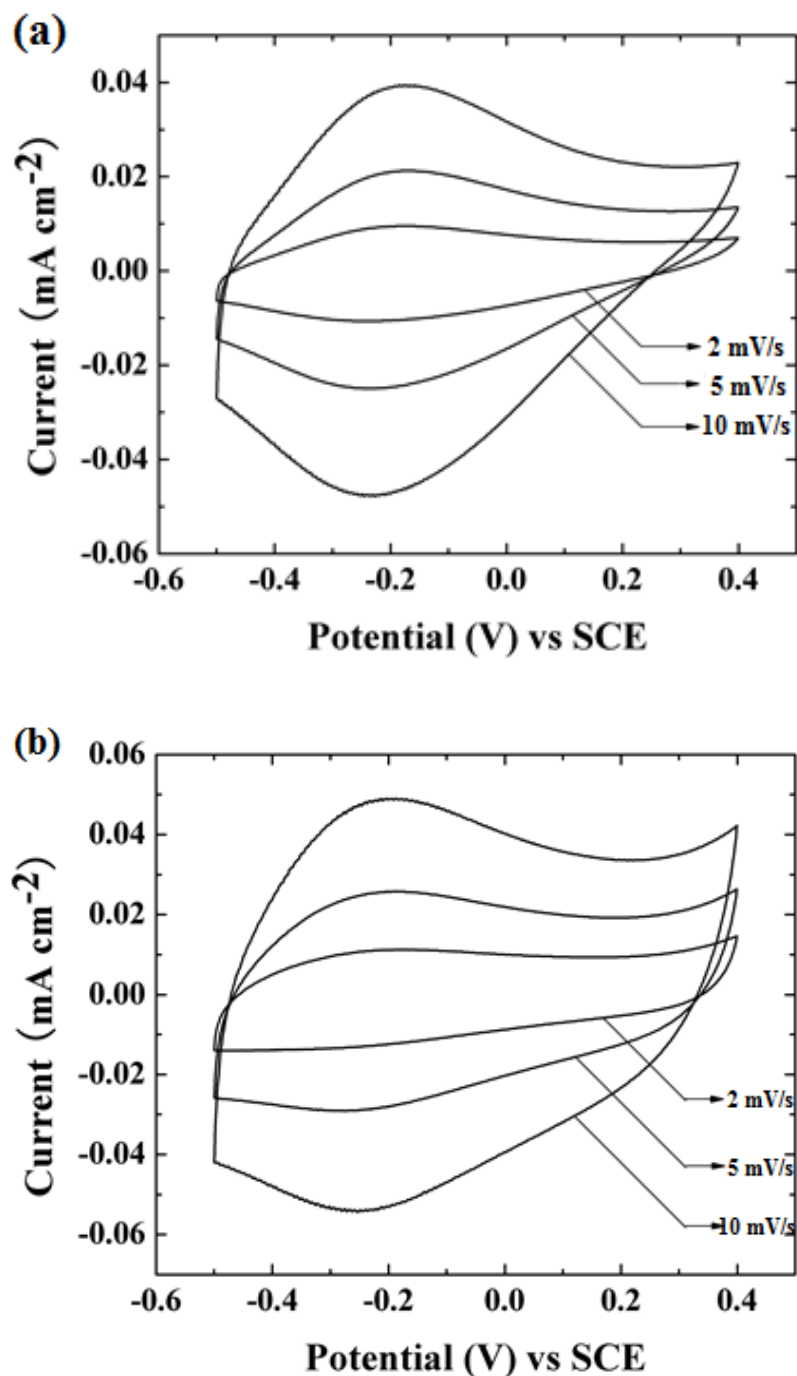


Figure 6-7 Cyclic voltammograms in 0.5 M Na₂SO₄ solution for 0.15 mg cm⁻² PPY film, prepared from the solution containing (a) 50 mM pyrrole and 5 mM CHR and (b) 100 mM pyrrole and 5 mM CHR.

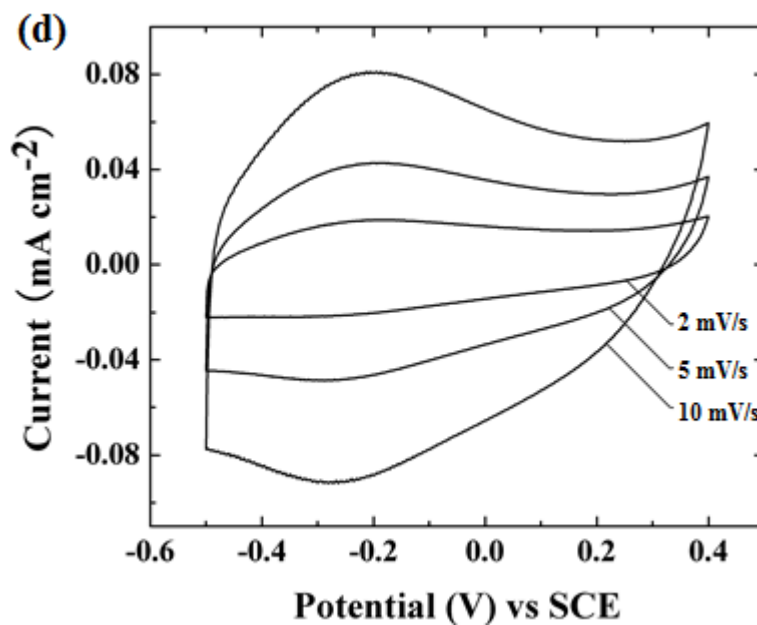
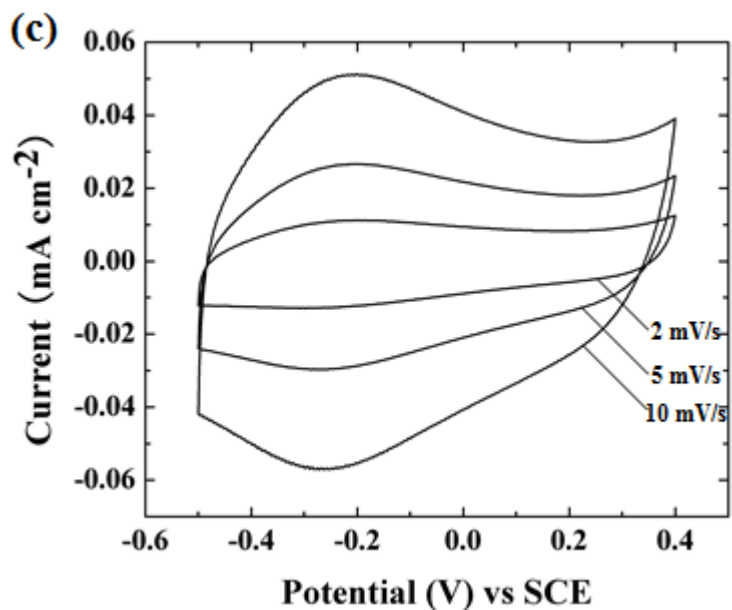


Figure 6-7 Cyclic voltammograms in 0.5 M Na₂SO₄ solution for 0.15 mg cm⁻² PPY film, prepared from the solution containing (c) 150 mM pyrrole and 5 mM CHR and (d) 150 mM pyrrole and 15 mM CHR.

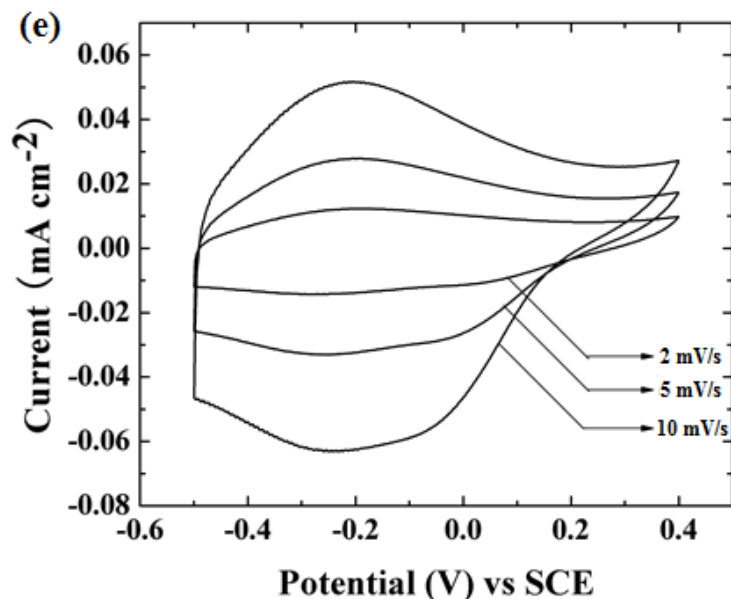


Figure 6-7 Cyclic voltammograms in 0.5 M Na₂SO₄ solution for 0.15 mg cm⁻² PPY film, prepared from the solution containing (e) 150 mM pyrrole and 50 mM CHR.

From the CVs, it was observed that the increase in concentration of CHR and pyrrole improves the shape of the curve at all scan rates. Ideal capacitive behavior was exhibited from the PPY films prepared from the solution containing higher concentration of CHR and Pyrrole (Fig 6-7 c, d, e) which results in higher SC.

As the electrochemical performance of PPY electrodes is strongly influenced by particle size, microstructure and porosity, the PPY films were studied by SEM. The films prepared from 150 mM pyrrole solution containing 5 mM CHR showed relatively low porosity with particle size below 0.5 μm (Figure 6-8 a). Similar images were obtained for the films prepared from 50 mM and 100 mM pyrrole solutions.

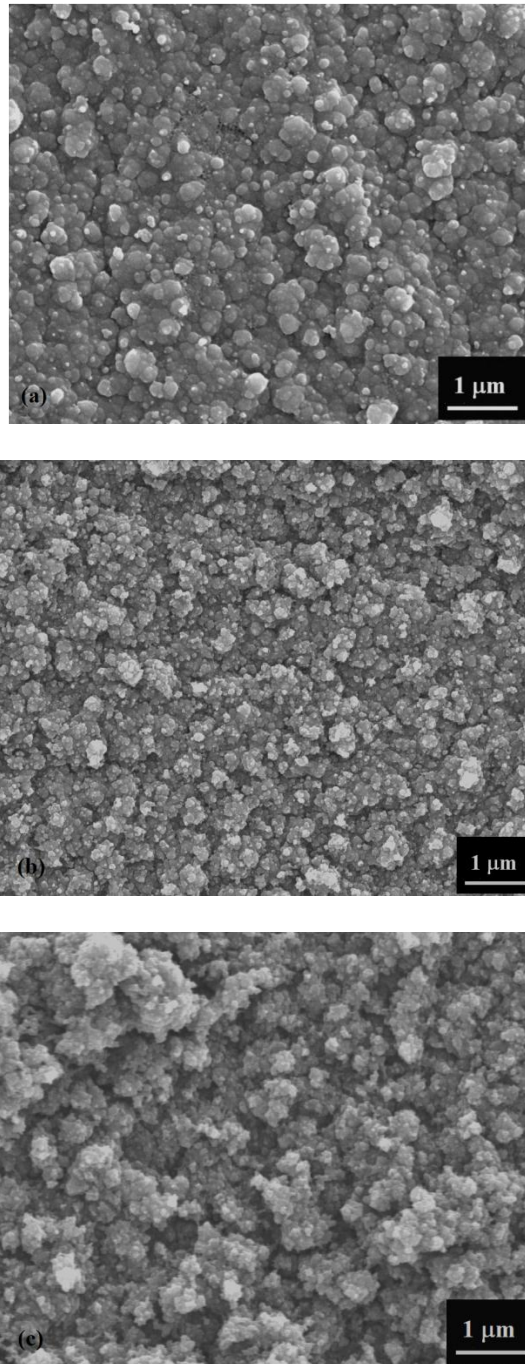


Figure 6-8 SEM images of films prepared from 150 mM pyrrole solution containing (a) 5, (b) 15 and (c) 50 mM CHR.

The disadvantageous aspect of low film porosity is that it leads to limited access to the interior sites of the polymer for dopant and electrolyte ions [93]. Low film porosity results in reduced SC, especially for thick films. The increase in CHR concentration in the solutions resulted in increased film porosity and finer size of individual particles (Figure 6-8 b,c).

Fig 6-13 shows the SC versus scan rates for the PPY films prepared from different concentrations of CHR and pyrrole. The films prepared from 50 mM pyrrole solutions containing 5mM CHR showed a SC of 208 Fg^{-1} at a scan rate of 2 mVs^{-1} . The SC decreased from 208 to 125 Fg^{-1} with increasing scan rate in the range of 2-100 mVs^{-1} (Figure6-9a). The decrease in the SC was attributed to diffusion limitation of the electrolyte in pores of the PPY film. The increase in the pyrrole concentration in the solutions in the range of 50-150 mM resulted in increase in SC (Figure6-9 b, c), which was especially evident at high scan rates. The films prepared from 150 mM pyrrole solutions containing 5 mM CHR showed SCs of 255 and 182 Fg^{-1} at scan rates of 2 and 100 mVs^{-1} , respectively. The increase in the CHR concentration in the solutions allowed further increase in SC (Figure6-9 d, e). The concentration range of CHR in solutions used for electropolymerization was limited by the solubility of this material in water. The highest SC of 343 Fg^{-1} was observed at 2 mVs^{-1} for the films prepared from the solutions containing 150 mM pyrrole and 50 mM CHR.

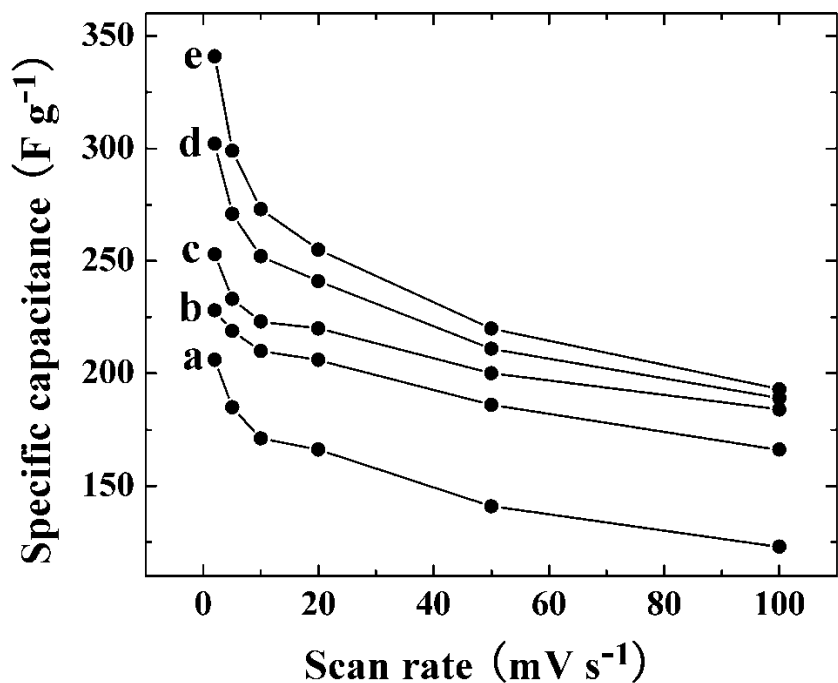


Figure 6-9 Specific capacitance versus scan rate for 0.1 mg cm^{-2} films prepared at current density of 1 mA cm^{-2} from (a) 50 mM pyrrole and 5mM CHR, (b) 100 mM pyrrole and 5mM CHR, (c) 150 mM pyrrole and 5 mM CHR , (d) 150 mM pyrrole and 15 mM CHR and (e) 150 mM pyrrole and 50 mM CHR.

6.1.3.3.2 Effect of film mass on Specific Capacitance

SC versus film mass for PPY films prepared at a constant current from the 100 mM pyrrole solutions containing 5 mM CHR at different scan rates is shown in Fig 6-10. It is interesting to notice that the SC increased with increasing specific mass of PPY films. The SC first increased with an increasing mass then decreased after a maximum value at

0.13 mg cm⁻² has been reached. The decrease of SC with increase of mass is attributed to the electrolyte diffusion limitations in the pores due to increasing film thickness. The increase of SC with increase of mass under 0.13 mg cm⁻² may be because of the very thin film thickness, such that the redox reaction involves entire polymer particles.

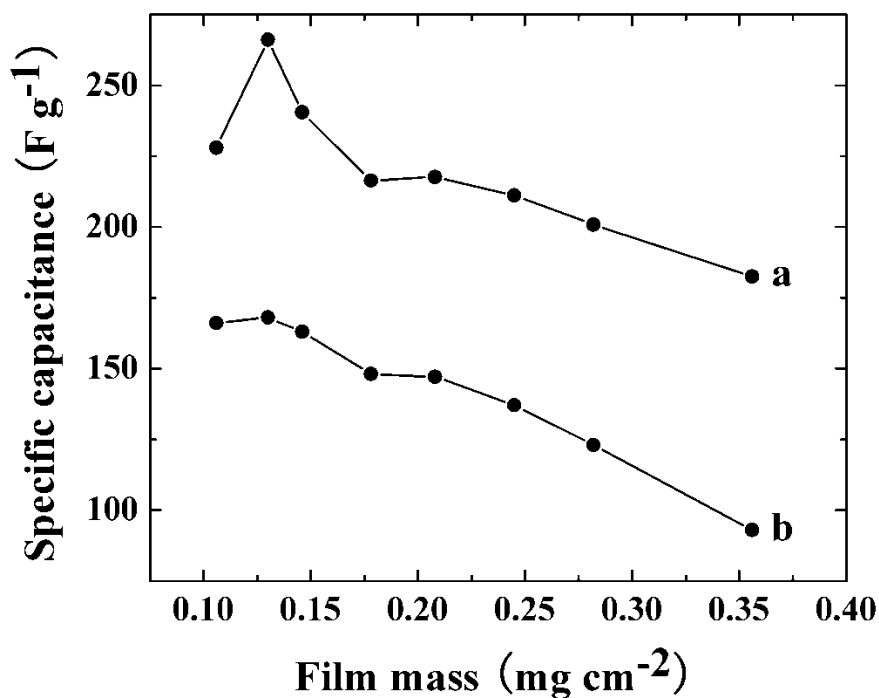


Figure 6-10 Specific capacitance at scan rates of (a) 2 and (b) 100 mV s⁻¹ versus mass of the films prepared from 100 mM pyrrole solutions containing 5 mM CHR.

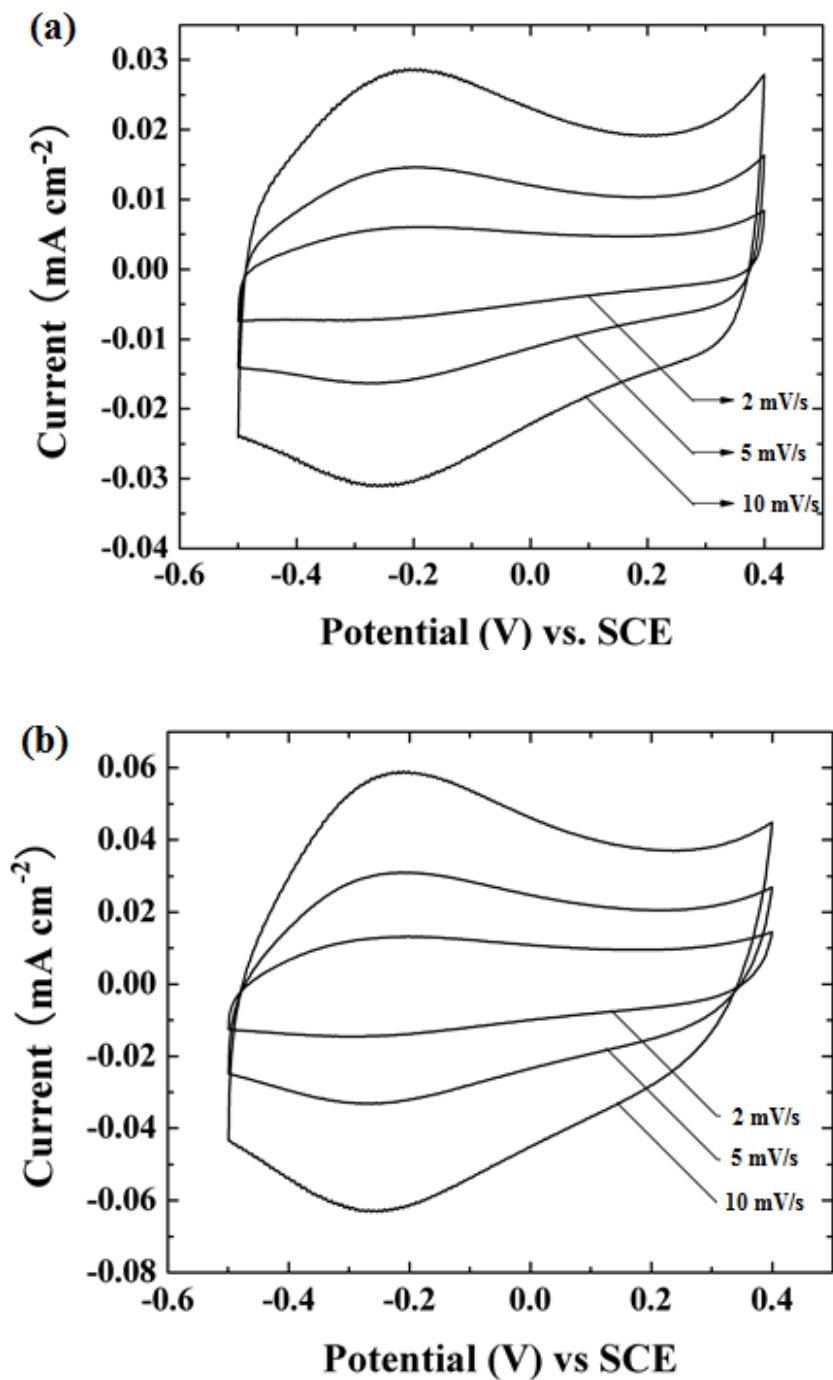


Figure 6-11 Cyclic voltammograms in 0.5 M Na₂SO₄ solution for PPY film, prepared from the solution containing 150 mM pyrrole and 5 mM CHR of film mass of (a) 0.096 mg cm⁻² and (b) 0.208 mg cm⁻².

6.1.3.3.3 Effect of Scan Rates on Specific Capacitance

The specific capacitance of PPY film of different specific masses as a function of scan rate is shown in Figure 6-12. The SC decreased with increasing scan rate. The decrease in the SC was attributed to diffusion limitation of the electrolyte in pores of the PPY film. This relatively high capacitance of PPY film can be attributed to the uniform porous structure and small polymer particle size which determined the ability of electrolyte ions to enter and to enable local ion transfer process.

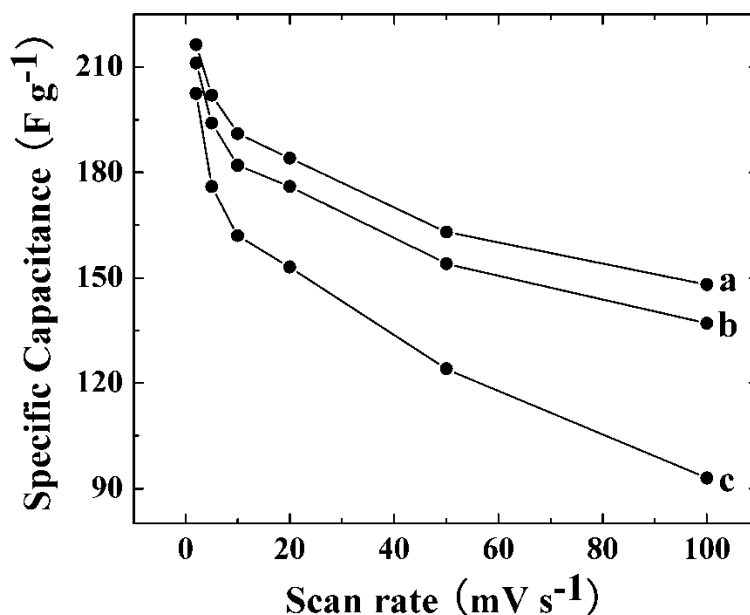


Figure 6-12 Specific capacitance versus scan rate for films of mass (a) 0.178 mg cm^{-2} , (b) 0.245 mg cm^{-2} and (c) 0.356 mg cm^{-2} prepared from (b) 5mM CHR and 100mM Pyrrole solution at current density of 1 mA cm^{-2} .

6.1.3.4 Electrochemical Impedance Spectra

The capacitive behavior of the PPY films is influenced by film morphology. Ionic conductivity and electronic conductivity of the electrode material influences the charge-discharge behavior of electrodes of ES. From the SEM investigations, PPY films prepared from high concentration of pyrrole and CHR exhibited high porosity compared to the PPY films prepared from low concentrations. It is suggested that the higher porosity of the PPY films result in a better electrolyte access to the active materials. This is in a good agreement with the further results of electrochemical impedance spectra (EIS) studies.

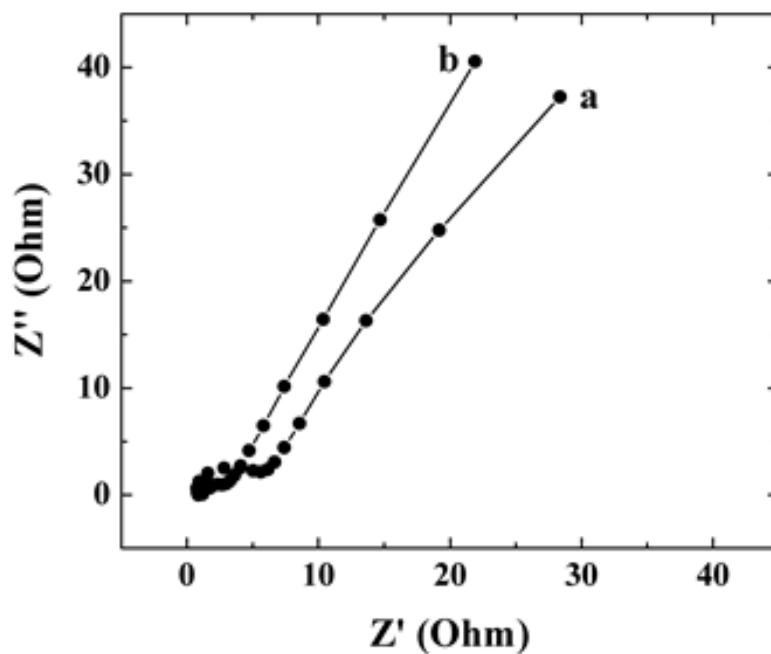


Figure 6-13 Nyquist plots for the 0.1 mg cm^{-2} films prepared at a current density of 1 mA cm^{-2} from the solution containing (a) 5 mM CHR and 50 mM Pyrrole, (b) 5 mM CHR and 150 mM Pyrrole.

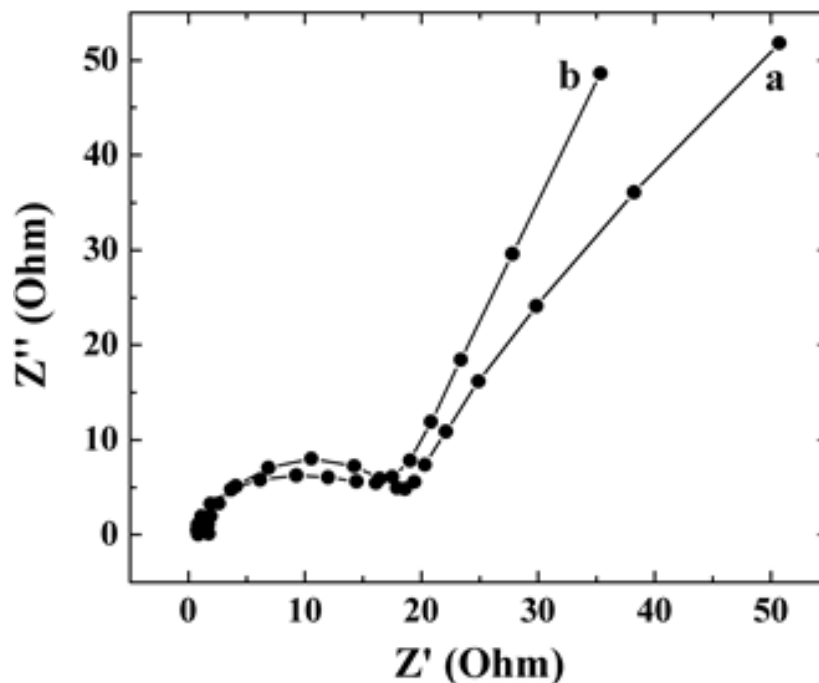


Figure 6-14 Nyquist plots for the 0.1 mg cm^{-2} films prepared at a current density of 1 mA cm^{-2} from the solution containing (a) 5 mM CHR and 150 mM Pyrrole, (b) 15 mM CHR and 150 mM Pyrrole.

Charge transfer and mass transport process occurring at the electrolyte/electrode interface and in active electrode materials can be obtained from EIS [89]. The series resistance can be measured from the Nyquist plot to calculate electronic and ionic conductivities of the electrochemical system. The summation of ohmic resistance of the electrolyte and/or electrode and a charge transfer resistance gives the total series resistance of the system [90]. The EIS curves for PPY films were obtained at open circuit potential (OCP) as shown in Fig 6-13 and Fig 6-14.

From the Nyquist plot as shown in the figure, two patterns are observed. A semi-circle region represents impedance at high frequencies and a linear region at lower

frequencies. The interfacial processes are represented by the arc from which the value of electrochemical charge transfer resistance can be evaluated, which is thought to be the main part of the resistance of ES [91]. The regions for both curves at low frequencies are relatively linear, indicating a capacitive behaviour related to the film charging mechanism. In Fig 6-13 and 6-14, the slope of the impedance curve for the PPY film prepared from high concentration of pyrrole and CHR at low frequencies is comparatively higher, indicating a better capacitive behaviour than that of the PPY film prepared from low concentrations. The capacitance could also be calculated from the low-frequency data of the EIS plot by the equation:

$$C = -1/(2\pi f Z_{\text{img}}) \quad (6-2)$$

Also the films prepared from high concentration of pyrrole and CHR have a much lower electrical resistance (Z') than that of the PPY films prepared from low concentration. The lower electrical resistance resulted in a higher SC. However, the capacitance evaluated from EIS was smaller than that calculated from the CV curve at low scanning rate due to the redox switching hysteresis of conducting polymer [91,92]. EIS data give a capacitance measured at a low voltage range, whereas CV data give a capacitance in the voltage window of 0.9 V.

The experimental EIS data could be simulated by using an appropriate electrical equivalent circuit (EEC) as shown in Fig 6-15, in order to analyze the electrochemical behaviour of the PPY film quantitatively. This equivalent circuit, included bulk resistance of electrolyte R_1 , resistance of film material R_2 , resistance of electrolyte R_3 and Warburgh impedance W in pores, and charge transfer resistance R_4 . The constant phase elements

represented the capacitance of the film material Q_1 and double layer capacitance in pores at the substrate-electrolyte interface Q_2 . The film of larger mass showed higher Z' values in the frequency range of 0.1 Hz-100 kHz. This was attributed to increase in R_2 , R_3 and W with increasing film thickness.

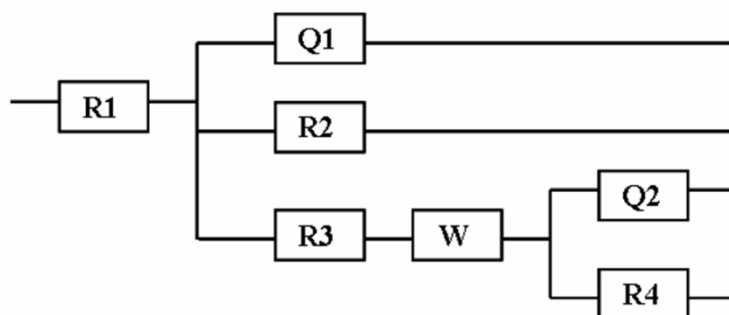


Figure 6-15 Equivalent circuit model for PPY electrode in a 0.5 M Na_2SO_4 electrolyte.

A good agreement between the experimental and calculated EIS data for PPY film was observed as shown in Fig 6-21. This fitting process verified that the proposed model can be used to simulate the electrochemical system for PPY films in a 0.5 M Na_2SO_4 electrolyte solution in the frequency range of 0.1 Hz-100k Hz. The decrease in SC was attributed to the increase in electrode resistance, which resulted from the increased film thickness and diffusion limitations in pores. This is in good agreement with the results of impedance measurements. Figure6-16 compares complex impedance $Z = Z' - iZ''$ for 0.18

and 0.36 mg cm^{-2} films deposited from the solution containing 100 mM pyrrole and 5 mM of CHR. It was found that at low frequencies, the slope of the curve for 0.36 mg cm^{-2} film was close to 45° , indicating significant contribution of Warburg impedance W . Film growth can result in reduced pore diameter, blockage of some pores and increased resistance in pores.

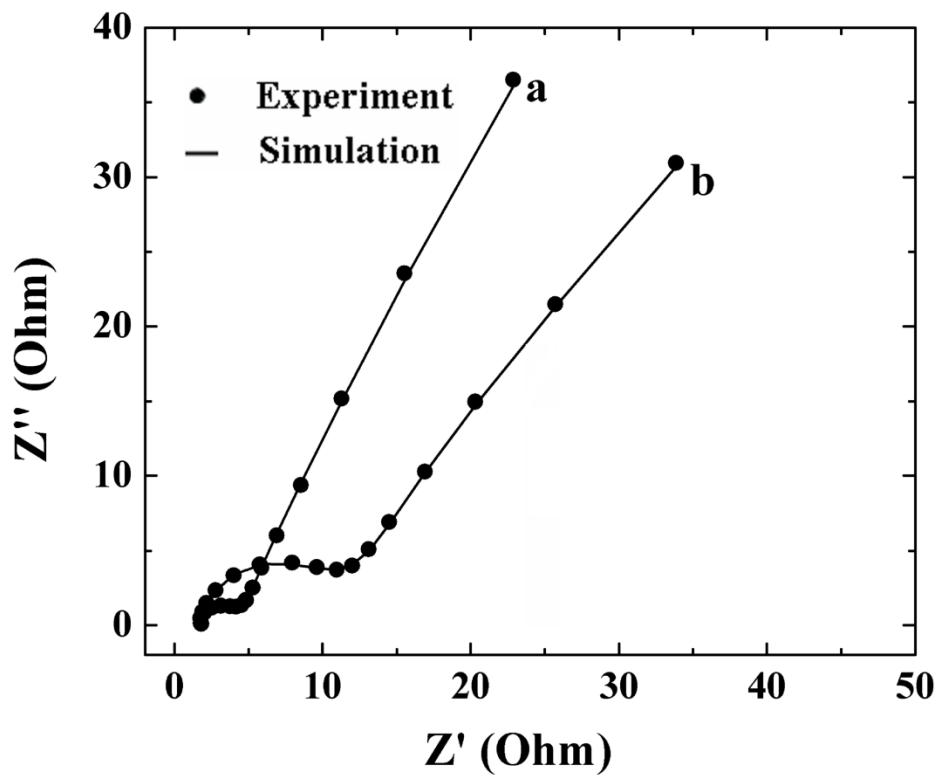


Figure 6-16 Nyquist plots of complex impedance $Z = Z' - iZ''$ for (a) 0.18 and (b) 0.36 mg cm^{-2} films deposited from the solution containing 100 mM pyrrole and 5 mM of CHR.

6.1.3.5 Cyclic Stability Test

The cyclic stability of the PPY films was investigated by continuous sweeping the potential for 1000 cycles between -0.5 - 0.4V at a scan rate of 50 mV s^{-1} . The CV of 1st and 1000th cycle is plotted as shown in Fig 6-17.

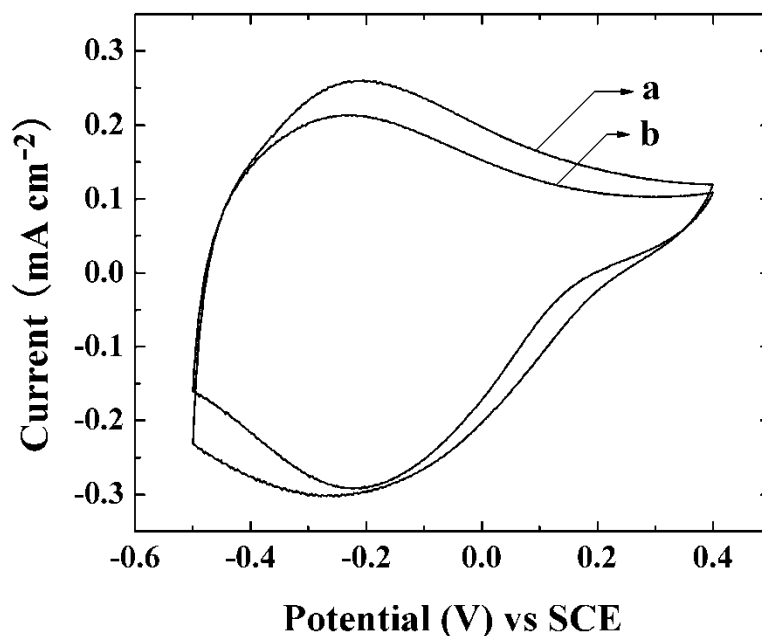


Figure 6-17 CV of the PPY film of mass 0.15 mg cm^{-2} recorded in the (a)1st and (b)1000th potential cycle at a scan rate of 50 mV s^{-1} in $0.5\text{M Na}_2\text{SO}_4$ electrolyte solution.

The PPY film shows significant changes in CV shape as well as area. The CV shape shifted inward in the potential range of -0.2 V - 0.3 V during the 1000th scan, and

the capacitive area become smaller after 1000th cycle indicating that the PPY film exhibits degradation.

The SC versus cycle number for the PPY films is shown in Fig 6-18. The SC decreased with an increasing cycle number. The decrease in SC values may be due to PPY degradation on swelling and shrinking in aqueous media and the PPY nanostructure may also change. The SC is decreased about 15% after 1000 cycles. The decrease in SC during cycling was also reported in other investigations [87,88].

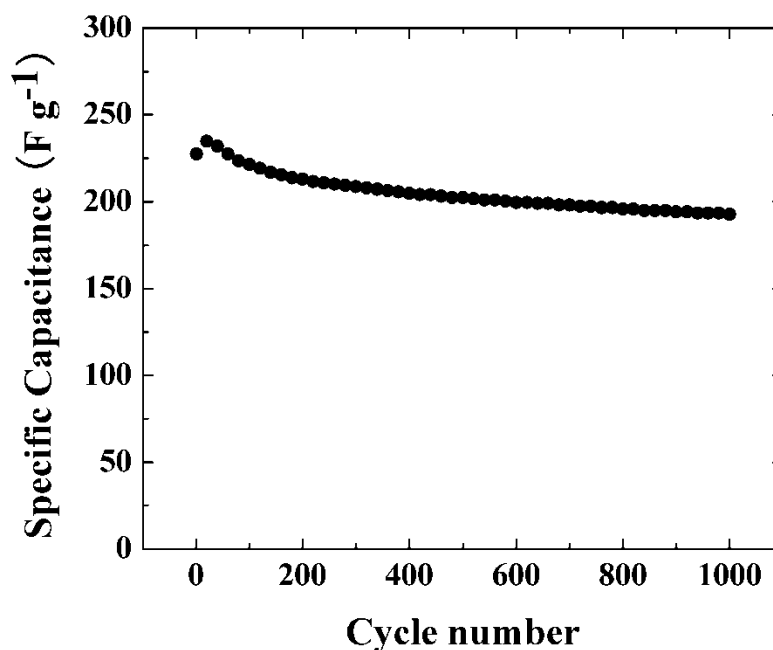


Figure 6-18 Specific capacitance versus cycle number at a scan rate of 50 mV s⁻¹ for 0.15 mg cm⁻² film prepared from the solution containing 150 mM pyrrole and 50 mM CHR.

The main strategies for improving cycle-life of PPY films include irradiation or compositing PPY with carbon nanotubes [87]. The improvement may be result of the relatively rigid incorporated carbon nanotubes which support and stabilize the porous structure of the composite against the influence of the repeated intercalation and removal of the charge balance ions. The stabilized porous structure can provide improved conductivity of composite.

6.1.3.6 Adhesion Test

The films prepared galvanostatically from pyrrole solution containing CHR were continuous, smooth and adhered well to the stainless steel substrates. The measurements of film adhesion according to the ASTM D3359 standard showed that adhesion strength corresponded to the 4B classification.

6.2 Electropolymerization of PPY doped with gallic acid

6.2.1 Potentiodynamic electropolymerization of PPY

The electropolymerization was performed to obtain PPY films on the stainless steel electrodes from aqueous solutions containing 5 mM gallic acid and 50 mM pyrrole under potentiodynamic conditions. The sweeps recorded during deposition are shown in Figure 6-19.

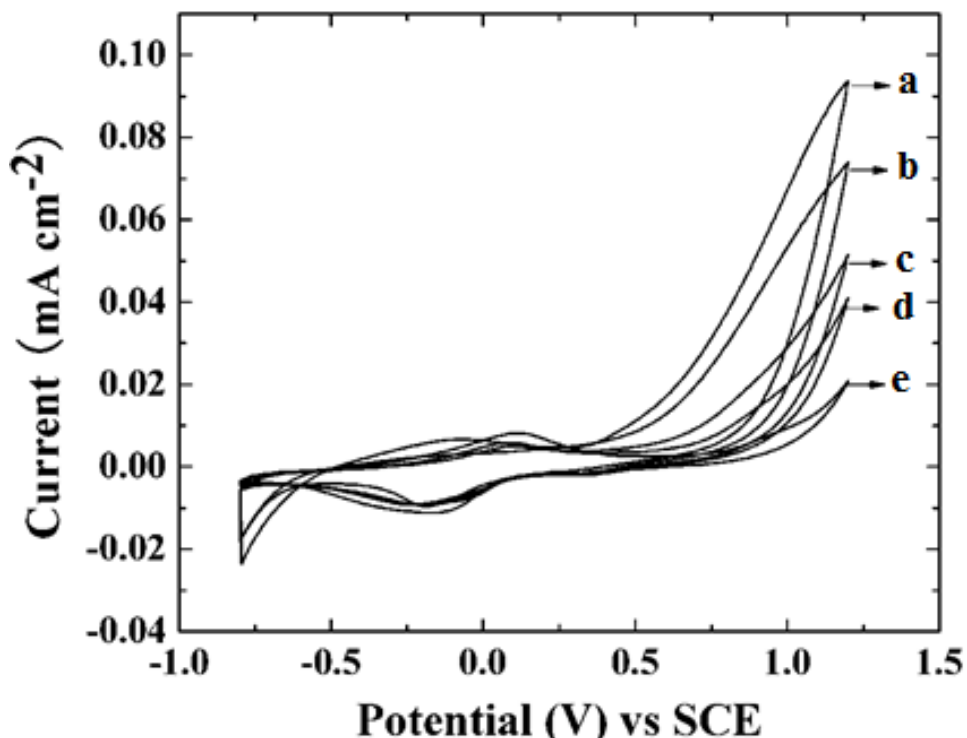


Figure 6-19 Cyclic voltammograms at (a) 1st cycle, (b) 2nd cycle, (c) 3rd cycle, (d) 4th cycle and (e) 10th cycle for stainless steel electrode in 50 mM pyrrole solution containing 5 mM Gallic acid at a scan rate of 20 mV s⁻¹.

Oxidation wave at ~ -0.15 V was observed during the first positive cycle, followed by a sharp increase in the anodic current. A rapid decrease of current was observed in the negative sweep and a reduction peak was observed at ~ -0.2 V. The oxidation peak was attributed to the formation of passive layer. It is suggested that gallic acid formed complexes with Fe (Figure 4.2) on the surface of the substrate and reduced the oxidation and dissolution rate. The complexation of gallic acid with Fe allowed the fabrication of PPY films on stainless steel. The sharp increase of current after oxidation peak indicated the formation of PPY film on the substrate since a black film was observed

on the electrode surface. The chain reaction of pyrrole units with cation radicals, and the polymerization on the metal surface resulted in the deposition of the polymer film. The oxidation peak disappeared during the next scan indicating that no chelating reaction occurred since the metal surface was covered by the PPY film formed in the first scan. The PPY film grew continuously on the repetitive sweep. The current decreased gradually with the number of scans since the conductivity of PPY is lower than the conductivity of the stainless steel substrates.

6.2.2 Galvanostatic electropolymerization of PPY

The PPY films were obtained on the anode at a constant current of 1 mA cm^{-2} from solutions containing 5 mM gallic acid and 50 mM pyrrole. The galvanostatic behaviour is shown in Figure 6-20. The potential–time curve is characterized by an induction peak curve followed by a plateau wave which represents the electropolymerization potential of PPY. Within the deposition time of 600 s, the black shiny deposit was achieved in the presence of gallic acid. It was observed that the oxidation potential is much higher than that when PPY is doped with CHR (Figure 6-3). The polymerization potential in the presence of gallic acid was 950 mV higher than that in the presence of CHR.

Since the less positive polymerization potential was beneficial to the formation of PPY, it was clear that CHR offers advantages for deposition of PPY film by minimizing the substrate corrosion and polymer over-oxidation. The formation of PPY was achieved due to the non-blocking passive layer formed by complexation with metal on the substrate

surface. It is suggested that adsorbed PPY acts as a charge transfer mediator during electropolymerization and promotes charge transfer.

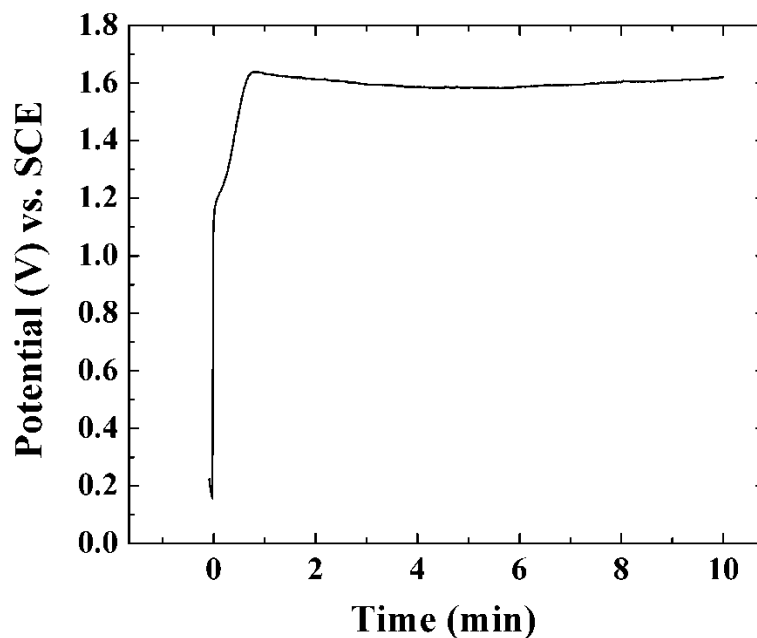


Figure 6-20 Potential versus time curves for galvanostatic deposition of PPY at a current density of 1mA cm^{-2} from 50 mM pyrrole solution in presence of 5 mM gallic acid.

6.2.3 Characterization of PPY film deposited using gallic acid

6.2.3.1 Deposit Mass characterization

Anodic polymerization from aqueous 250 mM pyrrole solutions containing 50 mM gallic acid resulted in the formation of strongly adherent films on the stainless steel substrate. Gallic acid (the chemical structure shown in Figure 4-2 a) was negatively

charged in the aqueous solutions due to the dissociation of $-\text{COOH}$ groups and served as anionic dopants. The anions were incorporated into the PPY matrix to ensure the electrical neutrality of the growing film during the anodic polymerization.

The film mass increased with increasing deposition time at a constant current density of 1 mA cm^{-2} condition as shown in Figure 6-21, indicating the formation of films of different thickness.

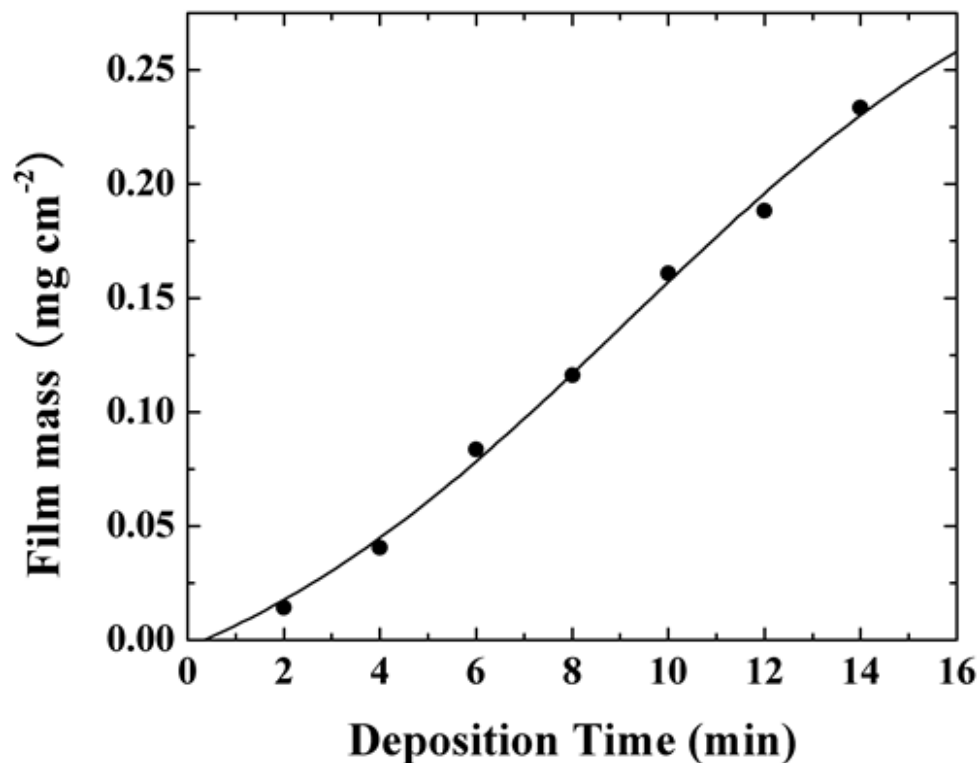


Figure 6-21 Film mass versus deposition time for films deposited from 250 mM pyrrole solution containing 50 mM gallic acid at a current density of 1 mA cm^{-2} .

6.2.3.2 Redox Reaction Properties

The electrochemical properties of the films were studied in a 0.5 M Na₂SO₄ solution using cyclic voltammograms (CV). PPY films were deposited at a constant current on stainless steel from the solution containing gallic acid whose concentration varied from 5 mM to 50 mM and pyrrole whose concentration varied from 50 mM to 250 mM. The concentration range of gallic acid and pyrrole in solutions used for electropolymerization was limited by the solubility of the materials in water. However, PPY films prepared from the solution containing low concentration of gallic acid and pyrrole showed poor adhesion and were non-uniform. Hence, films prepared from the solution containing 50mM gallic acid and 250 mM pyrrole were subjected to electrochemical tests. The films showed capacitive behaviour in the voltage window of 0.9 V. The area of CV increased with increasing scan rate. The anions of dissociated gallic acid participated in the charge-discharge by insertion and de-insertion from the matrix during the oxidation and reduction process. CVs of the PPY film doped with gallic acid of different film mass are shown in Figure 6-22, 6-23, 6-24. It was observed in all cases that ideal capacitive behaviour was not exhibited by the PPY films. Compared to the CVs of the PPY film doped with CHR, CVs of PPY film doped with gallic acid showed poor capacitive behaviour resulting in low specific capacitance. The redox reaction of the polymer can be expressed as shown in the Eq. 6-2.

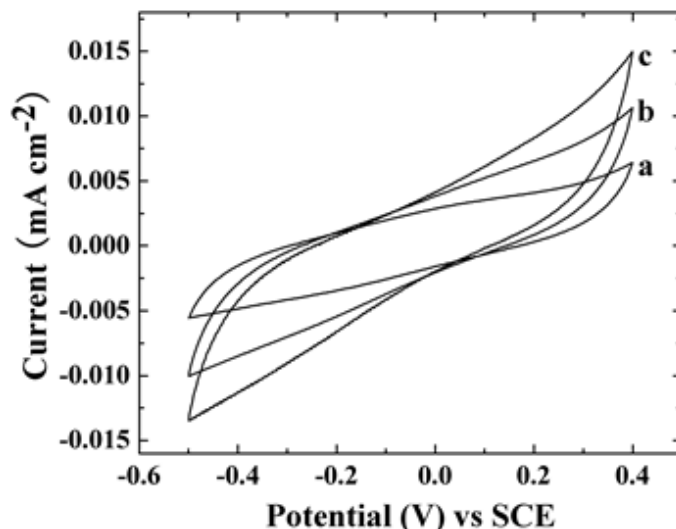


Figure 6-22 Cyclic voltammograms at scan rates of (a) 2, (b) 5 and (c) 10 mV s^{-1} for 0.083 mg cm^{-2} PPY film, prepared from the solution containing 250 mM pyrrole and 50 mM CHR.

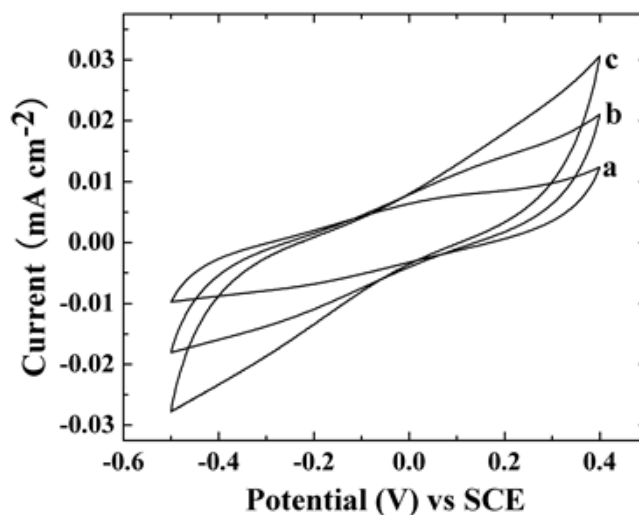


Figure 6-23 Cyclic voltammograms at scan rates of (a) 2, (b) 5 and (c) 10 mV s^{-1} for 0.116 mg cm^{-2} PPY film, prepared from the solution containing 250 mM pyrrole and 50 mM CHR.

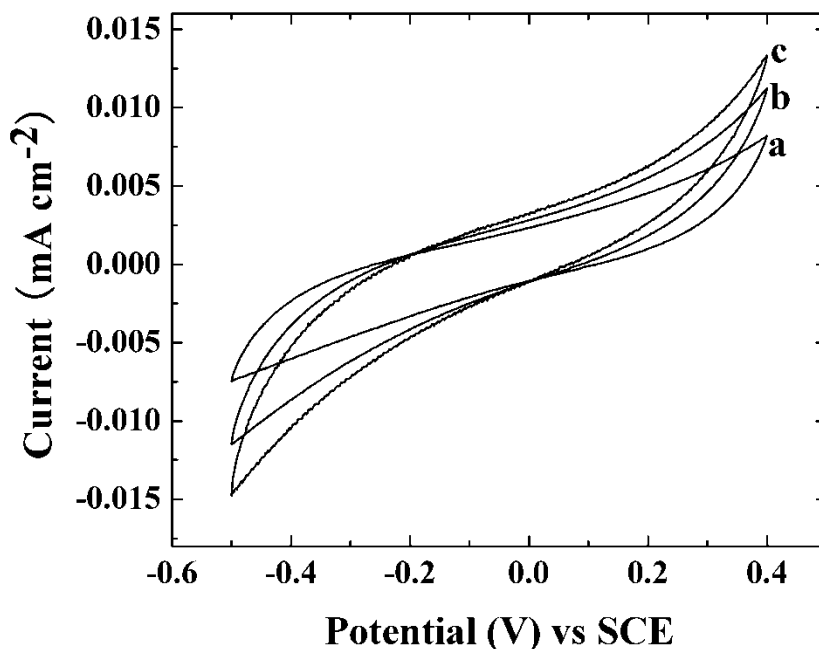


Figure 6-24 Cyclic voltammograms at scan rates of (a) 2, (b) 5 and (c) 10 mV s^{-1} in 0.5 M Na_2SO_4 solution for 0.188 mg cm^{-2} PPY film, prepared from the solution containing 250 mM pyrrole and 50 mM CHR.

6.2.3.3 Specific capacitance of PPY doped with Gallic acid

Figure 6-25 shows specific capacitance (SC) versus scan rate for the films of different thickness prepared from the pyrrole solutions containing gallic acid. The films showed SC in the range of 40 - 110 F g^{-1} at a scan rate of 2 mV s^{-1} . The SC decreased with increasing film thickness and increasing scan rate in the range of 2 - 100 mV s^{-1} . Such decrease is attributed to the limited penetration of electrolyte into the pores of PPY matrix and limited ions mobility within the pores.

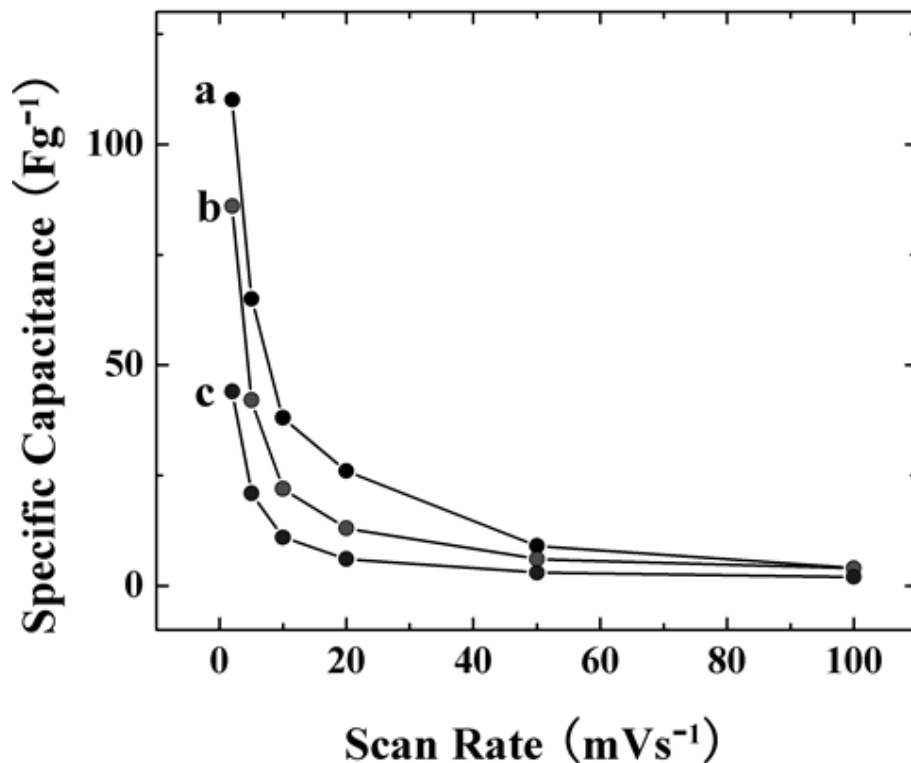


Figure 6-25 Specific capacitance versus scan rate for films of mass

(a) 0.083 mg cm^{-2} , (b) 0.116 mg cm^{-2} and (c) 0.188 mg cm^{-2} prepared from 50mM gallic acid and 250mM Pyrrole solution at current density of 1 mA cm^{-2} .

6.2.3.4 Electrochemical Impedance Spectra

EIS curves for PPY doped with Gallic acid were obtained at open circuit potential (OCP) as shown in Figure 6-26. EIS curves of PPY doped with gallic acid showed much higher resistance than that of PPY films doped with CHR. Hence, PPY films doped with gallic acid exhibited low capacitance which is in good agreement with CV results. PPY films doped with gallic acid showed lower resistance for films with low thickness and the resistance increased with increasing mass.

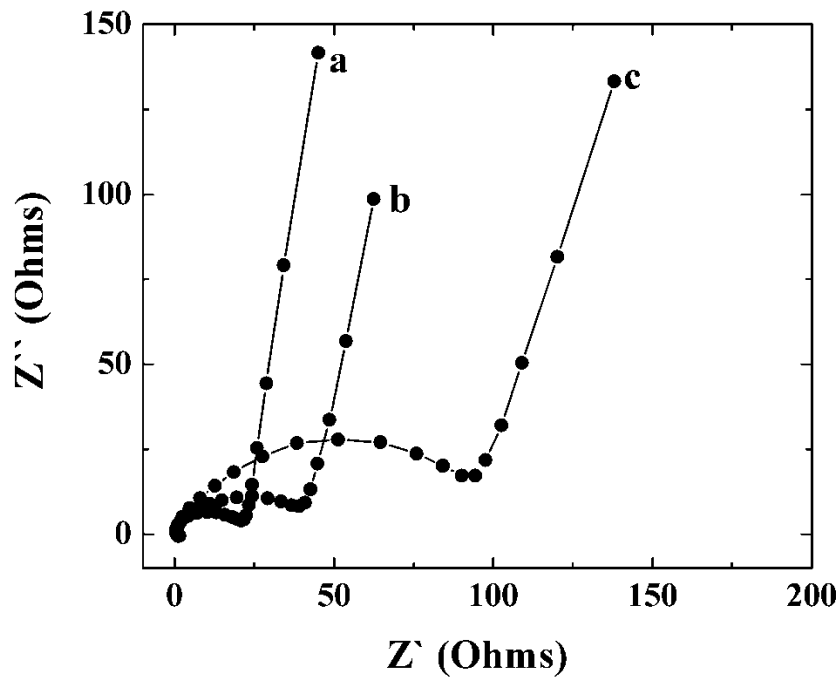


Figure 6-26 Nyquist plots for the films prepared at a current density of 1 mA cm^{-2} from the solution containing 50 mM Gallic acid and 250 mM Pyrrole with a film mass of (a) 0.083 mg cm^{-2} , (b) 0.116 mg cm^{-2} and (c) 0.188 mg cm^{-2} .

7 Conclusions

PPY films were obtained on stainless steel substrates by anodic electropolymerization using NSA, CHR and Gallic acid as anionic dopants. The deposition potential of PPY from the solutions containing CHR was lower than that for NSA and Gallic acid. Adherent and uniform PPY films were successfully obtained from pyrrole solutions containing CHR. The measurements of film adhesion according to the ASTM D3359 standard showed that adhesion strength corresponded to the 4B classification. The comparison of the experimental data for CHR, containing OH groups bonded to the aromatic rings, and NSA without OH groups showed that the interaction OH groups with metal atoms at the substrate surface promoted film adhesion. The deposition was performed galvanostatically or potentiodynamically. The film mass increased with increasing deposition time at a constant current density. Nearly linear dependence was observed, which indicated the possibility of deposition of films of controlled mass without induction time. The PPY films showed capacitive behaviour in the 0.5 M Na₂SO₄ electrolyte. PPY films doped with CHR showed better capacitive behaviour than that of PPY films doped with Gallic acid due to the presence of additional aromatic ring in CHR which enhances the conductivity of the PPY film. The SC increased with increasing pyrrole and CHR concentration in the solutions used for deposition. Electron microscopy investigations showed that the increase in SC with increasing CHR concentration can be attributed to decreasing particle size and increasing film porosity. The highest SC of 343 Fg⁻¹ was observed at 2 mVs⁻¹ for the films prepared from the solutions containing 150 mM pyrrole and 50 mM CHR. The SC decreased with

increasing scan rate. The SC decrease in thick films was attributed to increasing electrochemical impedance, which was analyzed at different frequencies using an equivalent circuit. The investigations of cycling stability of the films showed that the SC decreased by 15% after 1000 cycles. The PPY films prepared on stainless steel substrates by electropolymerization are promising electrode materials for ES.

References

- [1] B. Viswanathan, "Energy sources," An introduction to energy sources, 2006.
- [2] B.E.Conway, *Electrochemical Supercapacitors: Scientific Fundamentals and Technological Applications*. New York, N.Y.: Kluwer Academic, 1999.
- [3] A. G. Pandolfo and A. F. Hollenkamp, ‘ Carbon Properties and Their Role in Supercapacitors’, *Journal of Power Sources*, 157 (2006): p1539.
- [4] R. J. Brodd, A. Kozawa and K. V. Kordesch, ‘Primary Batteries 1951 – 1976’, *Journal of the Electrochemical Society*, 125 (1978): p271c.
- [5] R. Kotz, Carlen, M., “Principles and applications of electrochemical capacitors” *Electrochimica Acta*, vol. 45, pp. 2483-2498, 2000.
- [6] P. P. Barker, “Ultracapacitors for use in power quality and distributed resource Applications”, *presented at IEEE PES Summer Meeting, 21-25 July 2002, Piscataway, NJ, USA, 2002.*
- [7] P. Simon, Y. Gogosti, “Materials for electrochemical capacitors” in *Nature Materials*, vol. 7, pp. 845-854, 2008.
- [8] T. C. Murphy, R. B. Wright, R., “Electrochemical capacitors II” Proceedings, vols. 96-25, *The Electrochemical Society, Pennington, NJ*, pp.258, 1997.
- [9] L. T. Lam, R. Louey, “Development of ultra-battery for hybrid-electric vehicle Applications” *Journal of Power Sources*, vol. 158, pp. 1140-1148, 2006.
- [10] F. S. Garcia, A. A. Ferreira, J. A. Pomilio, “Control Strategy for battery-Ultracapacitor hybrid energy storage system” presented at *2009 Twenty-Fourth Annual IEEE Applied Power Electronics Conference and Exposition (APEC)*, 15-19 Feb. 2009, *Piscataway, NJ, USA, 2009.*
- [11] R. Kotz, Carlen, M., “Hybrid Power – A fuel cell car boosted with Supercapacitors”, 2002.

- [12] Burke, A. "Ultracapacitors: why ,how, and where is the technology", *Journal Of Power Sources* 91, 37-50 (2000).
- [13] A. K. Shukla, S. Sampath, K., "Electrochemical Supercapacitors: Energy Storage beyond Batteries", *Current Science*, 79, pp1656, 2000.
- [14] Y. Zhang, H. Feng, X., "Progress of electrochemical capacitor electrode material" *International journal of hydrogen energy*, vol. 34, pp. 4889-4899, 2009.
- [15] B. E. Conway, W. G. Pell, "Double-layer and psuedocapacitance types of Electrochemical capacitors and their applications to the development of hybrid Devices" *Journal of Solid State Electrochemistry*, vol. 7, pp. 637-644, 2003.
- [16] Halper, M. S. & Ellenbogen, "Supercapacitor: A brief overview", *MITRE*, March 2006.
- [17] Probstle, H., Wiener, M. & Fricke, "Carbon Aerogels for Electrochemical Double Layer Capacitors", *Journal of Porous Materials*, vol. 10, pp. 213-222, 2003.
- [18] Probstle, H., Schmitt, C. & Fricke, "Button cell supercapacitors with monolithic Carbon aerogels", *Journal of Power Sources*, vol. 105, pp. 189-194, 2002.
- [19] Y. Y. Fan, A. Kaufmann, A., "Single- and multi-wall carbon nanotubes produced Using floating catalyst method: Synthesis, purification and hydrogen up-take", *Carbon*, vol. 44, pp. 2160-2170, 2006.
- [20] W. K. Maser, A. M. Benito, "Production of carbon nanotubes: the light approach" *Carbon*, vol. 40, pp. 1685-1695, 2002.
- [21] E. Frackowiak, "Nanotubular materials as electrodes for supercapacitors", *Fuel Processing Technology*, vol. 77-78, pp. 213-219, 2002.
- [22] E. Frackowiak, "Enhanced capacitance of carbon nanotubes through chemical activation" *Chemical Physics Letters*, vol. 361, pp. 35-41, 2002.
- [23] Q. Jiang, "A study of activated carbon nanotubes as electrochemical super capacitors electrode materials" *Materials Letters*, vol. 57, pp. 988-991, 2002.

- [24] C. Peng, S. Zheng, D., "Carbon nanotube and conducting polymer composites for supercapacitors", *Progress in Natural science*, vol. 18, pp. 777, 2008.
- [25] A. B. Patrice Simon, "Nanostructured carbons: double-layer capacitance and more" *The Electrochemical Society Interface*, vol. 17, pp. 38-43, 2008.
- [26] R. Niessen, "Electrochemical hydrogen storage in lightweight electrode materials", *Ph.D. thesis, Technische Universiteit Eindhoven (2006)*.
- [27] P. Simon & Y. Gogosti, "Materials for electrochemical capacitors" *Nature Materials*, vol.7, pp. 845-854, 2008.
- [28] C. C. Hu, M.J. Liu, K., "Anodic deposition of hydrous ruthenium oxide for supercapacitors" *Journal of Power Source*, vol.163, pp. 1126-1131, 2007.
- [29] J.J. Jow, H.J. Lee, H.R. Chen, M.S. Wu, T.Y. Wei, "Anodic, cathodic and cyclic voltammetric deposition of ruthenium oxides from aqueous RuCl₃ solutions" *Electrochimica Acta*, vol. 52, pp. 2625-2633, 2007.
- [30] B. J. Lee, "Carbon nanofibre/hydrous RuO₂ nanocomposite electrodes for supercapacitors" *Journal of Power Sources*, vol. 168, pp. 546-552, 2007.
- [31] S.H. Lee, P. Liu, H. M. Cheong, C. E. Tracy, S. K. Deb, "Electrochromism of amorphous ruthenium oxide thin films," *Solid State Ionics*, vol. 165, pp. 217-221, 2003.
- [32] X. Qin, "Electrochemical characterization on Ru_nO₂·xH₂O/carbon nanotubes composite electrodes for high energy density supercapacitors" *Carbon*, vol. 42, pp. 451-453, 2004.
- [33] I.H. Kim , K.B. Kim, "Electrochemical Characterization of Hydrous Ruthenium Oxide Thin-Film Electrodes for Electrochemical Capacitor Applications" *Journal of The Electrochemical Society*, vol. 153, pp. A383-A389, 2006.
- [34] J.P. Zheng and T.R. Jow, "A New Charge Storage Mechanism for Electrochemical Capacitors", *Journal of the Electrochemical Society*, vol.142, pp. L6, 1995.

- [35] M. Jayalakshmi and K. Balasubramanian, "Simple capacitors to Supercapacitors – An Overview", *International Journal of Electrochemical Science*, vol.3, pp. 1196-1217, 2008.
- [36] V. Srinivasan and J.W. Weidner, "Capacitance Studies of Cobalt Oxide Films Formed via Electrochemical precipitation", *Journal of Power Sources*, vol. 108, pp. 15, 2005.
- [37] S.G. Kandalkar, J.L. Gunjekar, C., "Preparation of cobalt oxide thin films and its use in supercapacitor application", *Applied Surface Science*, vol. 254, pp. 5540-5544, 2008
- [38] K. Liu and M.A. Anderson, "Porous nickel oxide/nickel films for electrochemical capacitors", *Journal of the Electrochemical Society*, vol.143, pp. 124-130, 1996.
- [39] V. Srinivasan and J.W. Weidner, "An electrochemical route for making porous nickel oxide electrochemical capacitors", *Journal of the Electrochemical Society*, vol.144, pp. 210-213, 1997.
- [40] K. Nam, K. Kim, "A study of the preparation of NiOx electrode via electrochemical route for supercapacitor applications and their charge storage mechanism", *Journal of the Electrochemical Society*, vol.149, pp. A346-A354, 2002.
- [41] S. W. Z. a. G. Z. Chen, "Manganese oxide based materials for supercapacitors," *Energy Materials :materials science and engineering for energy systems*, vol. 3, pp. 186-200, 2008.
- [42] J. Wei, I. Zhitomirsky, "Manganese oxide films for electrochemical supercapacitors" *Journal of Materials Processing Technology*, vol. 186, pp. 356-361, 2007.
- [43] P. Staiti, F. Lufrano, "Study and optimization of manganese oxide-based electrodes for electrochemical supercapacitors" *Journal of Power Sources*, vol. 187, pp. 284-289, 2009.

- [44] C.Y. Chen, "Hybrid manganese oxide films for supercapacitor application prepared by sol-gel technique" *Thin Solid Films*, vol. 518, pp. 1557-1560, 2009.
- [45] B.E. Conway, *Electrochemical Supercapacitors: Scientific Fundamentals and Technological Applications*. New York, N.Y.: Kluwer Academic, 1999
- [46] K.S. Ryu, Y.G. Lee, Y., "Poly(ethylenedioxythiophene) (PEDOT) as Polymer Electrode in Redox Supercapacitors", *Electrochimica Acta*, vol 50, pp.843, 2004.
- [47] K. S. Ryu, X. Wu, Y.G. Lee, S. H. Chang, "Electrochemical capacitor composed of doped polyaniline and polymer electrolyte membrane" *Journal of Applied Polymer Science*, vol. 89, pp. 1300-1304, 2003.
- [48] K.W. Nam and K.B. Kim, "Manganese oxide film electrodes prepared by electrostatic spray deposition for electrochemical capacitors", *Journal of the Electrochemical Society*, vol 153, pp. 81-88, 2006.
- [49] N. G. Sahoo, S. Rana, J. W. Cho, L. Li, S. H. Chan, "Polymer nanocomposites based on functionalized carbon nanotubes" *Progress in Polymer Science*, vol. In Press, Corrected Proof, 2010.
- [50] B. Du, Q. Jiang, X. F. Zhao, B. Huang, Y. Zhao, "Preparation of PPY/CNT composite applications for supercapacitor electrode material" *Materials Science Forum*, pp. 502-5, 2009.
- [51] X. Zhang, W. Yang, Y. Ma, "Synthesis of polypyrrole-intercalated layered manganese oxide nanocomposite by a delamination/reassembling method and its electrochemical capacitance performance" *Electrochemical and Solid-State Letters*, vol. 12, pp. A95-A98, 2009.
- [52] W. Sugimoto, K. Yokoshima, Y., "Charge storage mechanism of nanostructured Anhydrous and hydrous ruthenium based oxides" *Electrochimica Acta*, vol. 52, pp. 1742, 2006.

- [53] H. Y. Lee and J. B. Goodenough, "Supercapacitor behaviour with KCl electrolyte", *Journal of Solid State Chemistry*, vol. 144, pp. 220, 1999.
- [54] M. Toupin, T. Brousse and D. Belanger, "Charge storage mechanism of MnO₂ Electrode used in aqueous electrochemical capacitor", *Chemistry of Materials*, Vol. 16, pp. 3184, 2004.
- [55] X. Xie and L. Gao, "Characterization of a manganese dioxide/carbon nanotube Composite fabricated using an in situ coating method", *Carbon*, vol. 45, pp. 2365, 2007.
- [56] E. Frackowiak, G. Lota, J., "Room-temperature phosphonium ionic liquids for Supercapacitor applications", *Applied Physics Letters*, vol. 86, pp. 164104, 2005.
- [57] J. M. Pringle, O. Ngamna, J. Chen, G. G. Wallace, M. Forsyth, D. R. MacFarlane, "Conducting polymer nanoparticles synthesized in an ionic liquid by chemical polymerisation" *Synthetic Metals*, vol. 156, pp. 979-983, 2006.
- [58] D. D. Borole, U. R. Kapadi, P. P. Mahulikar, D. G. Hundiwale, "Electrochemical synthesis and characterization of conducting copolymer: Poly(o-aniline-co-o-toluidine)" *Materials Letters*, vol. 60, pp. 2447-2452, 2006.
- [59] N. K. Guimard, N. Gomez, C. E. Schmidt, "Conducting polymers in biomedical engineering" *Progress in Polymer Science, Polymers in Biomedical Applications*, vol. 32, pp. 876-921, 2007.
- [60] M. Omastová, K. Mosnácková, M. Trchová, E. N. Konyushenko, J. Stejskal, P. Fedorko, J. Prokes, "Polypyrrole and polyaniline prepared with cerium(IV) sulfate oxidant," *Synthetic Metals*, vol. 160, pp. 701-707, 2010.
- [61] M. M. Castillo-Ortega, M. B. Inoue, M. Inoue, "Chemical synthesis of highly conducting polypyrrole by the use of copper(II) perchlorate as an oxidant," *Synthetic Metals*, vol. 28, pp. 65-70, 1989.

- [62] B. L. Funt and A. F. Diaz, "Organic electrochemistry: An Introduction and a Guide", *Marcel Dekker, New York, pp. 1337, 1991.*
- [63] J. L. Bredas, "Bipolarons in doped conjugated polymers: a critical comparison between theoretical results and experimental data" *Molecular Crystals and Liquid Crystals, vol. 118, pp. 49-56, 1985.*
- [64] S. Wencheng and J. O. Iroh, "Electrodeposition mechanism of polypyrrole Coatings on steel substrate from aqueous oxalate solution", *Electrochimica Acta, vol. 46, pp. 1-8, 2000.*
- [65] J. Ouyang, Y. Li, "Effect of electrolyte solvent on the conductivity and structure of as-prepared polypyrrole films," *Polymer, vol. 38, pp. 1971-1976, 1997.*
- [66] L. F. Warren, D. P. Anderson, "Polypyrrole Films from Aqueous Electrolytes" *Journal of The Electrochemical Society, vol. 134, pp. 101-105, 1987.*
- [67] U. Johanson, M. Marandi, T. Tamm, J. Tamm, "Comparative study of the behavior of anions in polypyrrole films" *Electrochimica Acta, vol. 50, pp. 1523-1528, 2005.*
- [68] A. A. A. Almario, R. L. T. Cáceres, "Study of kinetic formation and the electrochemical behavior of polypyrrole films" *Journal of the Chilean Chemical Society, vol. 54, pp. 14-19, 2009.*
- [69] G. Sabouraud, S. Sadki, N. Brodie, "The mechanisms of pyrrole electropolymerization " *Chemical Society Reviews, vol. 29, pp. 283-293, 2000.*
- [70] W. Su, J. O. Iroh, "Electrodeposition mechanism, adhesion and corrosion performance of polypyrrole and poly(N-methylpyrrole) coatings on steel substrates" *Synthetic Metals, vol. 114, pp. 225-234, 2000.*
- [71] S. U. Rahman, M. S. Ba-Shammakh, "Thermal effects on the process of electropolymerization of pyrrole on mild steel" *Synthetic Metals, vol. 140, pp. 207-223, 2004.*

- [72] C. M. Li, C. Q. Sun, W. Chen, L. Pan, "Electrochemical thin film deposition of polypyrrole on different substrates" *Surface and Coatings Technology*, vol. 198, pp. 474-477, 2005.
- [73] J.H. Waite, "Mussel power", *Nature Material*, vol. 7, pp. 8, 2008.
- [74] P.A. Connor, K.D. Dobson, A.J. McQuillan, "New Sol-Gel Attenuated Total Reflection Infrared Spectroscopic Method for Analysis of Adsorption at Metal Oxide Surfaces in Aqueous Solutions. Chelation of TiO₂, ZrO₂, and Al₂O₃ Surfaces by Catechol, 8-Quinolinol, and Acetylacetone", *Langmuir* vol. 11, pp. 4193, 1995.
- [75] W. Huang, P. Jiang, C. Wei, D. Zhuang, and J. Shi, "Low-Temperature One-Step Synthesis of Covalently Chelated ZnO/Dopamine Hybrid Nanoparticles and their Optical Properties", *Journal of Materials Research*, vol. 23 [7], pp. 1946, 2008.
- [76] T. Rajh, L. X. Chen, K. Lukas, T. Liu, M. C. Thurnauer, and D. M. Tiede, "Surface Restructuring of Nanoparticles: An Efficient Route for Ligand-Metal Oxide Crosstalk", *Journal of Physical Chemistry B*, vol. 106, pp. 10543, 2002.
- [77] Guang-Li Wang, Jing-Juan Xu, Hong-Yuan Chen, "Dopamine sensitized nanoporous TiO₂ film on electrodes: Photoelectrochemical sensing of NADH under visible irradiation", *Biosensors and Bioelectronics*, vol. 24, pp. 2494, 2009.
- [78] P.Z. Araujo, P.J. Morando and M.A. Blesa, "Interaction of Catechol and Gallic Acid with Titanium Dioxide in Aqueous Suspensions. 1. Equilibrium Studies", *Langmuir*, vol. 21, pp. 3470, 2005.
- [80] I.A. Jankovic, Z.V. Saponjic, M.I. Cornor, J.M. Nedeljkovic, *Journal of Physical Chemistry C*, vol. 113, pp. 12645, 2009.

- [81] K. Wu, Y. Wang, I. Zhitomirsky, "Electrophoretic deposition of TiO₂ and composite TiO₂-MnO₂ films using benzoic acid and phenolic molecules as charging additives" *Journal of Colloid and Interface Science*, vol. 352, pp. 371, 2010.
- [82] Y. Wang, I. Zhitomirsky, "Effect of phenolic molecules on electrophoretic deposition on manganese dioxide-carbon nanotube nanocomposites" *Colloids and Surfaces A*, vol. 369, pp. 211, 2010.
- [83] D. E. Tallman, C. Vang, G. G. Wallace, G. P. Bierwagen, "Direct electrodeposition of polypyrrole on aluminum and aluminum alloy by electron transfer mediation" *Journal of the Electrochemical Society*, vol. 149, pp. C173-C179, 2002.
- [84] D. O. N. Yan Wang, "An investigation into the nucleation and growth of an electropolymerized polypyrrole coating on a 316L stainless steel surface" *Thin Solid Films*, vol. 516, pp. 7427-7432, 2008.
- [85] R. Ansari Khalkhali, "Electrochemical Synthesis and Characterization of Electroactive Conducting Polypyrrole Polymers" *Russian Journal of Electrochemistry*, vol. 41, pp. 950-955, 2005.
- [86] R. Zhu, G. Li, G. Huang, "Two-step electrosynthesis of polypyrrole for corrosion protection of stainless steel" *Materials and Corrosion*, vol. 60, pp. 34-39, 2009.
- [87] G.A. Snook, P. Kao, A.S. Best, "Conducting-polymer-based supercapacitor devices and electrodes", *Journal of Power Sources*, vol. 196, pp. 1-12, 2011.
- [88] L.-Z. Fan, J. Maier, "High-performance polypyrrole electrode materials for redox Supercapacitors", *Electrochemistry Communications* vol. 8, pp. 937-940, 2006.
- [89] S. O. Arash Shahryar, Jerzy A. Szipunar, "Enhancement of biocompatibility of 316LVM stainless steel by cyclic potentiodynamic passivation" *Journal of Biomedical Materials Research Part A*, vol. 89A, pp. 1049-1062, 2009.

- [90] Y. a. Q. Li, Renyuan, "Studies on the electrode kinetics of polypyrrole in aqueous solution by a.c. impedance measurement" *Synthetic Metals*, vol. 64, pp. 241-245, 1994.
- [91] J. Wang, Y. Xu, X. Chen, X. Sun, "Capacitance properties of single wall carbon nanotube/polypyrrole composite films" *Composites Science and Technology, Polymer Nanocomposites - Modeling, Mechanical and Functional Properties – Polymer Nanocomposites*, vol. 67, pp. 2981-2985, 2007.
- [92] R. Hass, J. García-Cañadas, G. Garcia-Belmonte, "Electrochemical impedance analysis of the redox switching hysteresis of poly(3,4-ethylenedioxythiophene) films" *Journal of Electroanalytical Chemistry*, vol. 577, pp. 99-105, 2005.
- [93] S. A. Campbell, Y. Li, S. Breakspear, F. C. Walsh, J. R. Smith, "Conducting polymer coatings in electrochemical technology. Part 1 - synthesis and fundamental aspects" *Transactions of the Institute of Metal Finishing*, vol. 85, pp. 237-44, 2007.
- [94] K. Meerholz, J. Heinze, "Influence of chain length and defects on the electrical conductivity of conducting polymers" *Synthetic Metals*, vol. 57, pp. 5040-5045, 1993.
- [95] K. Gurunathan, A. V. Murugan, R. Marimuthu, U. P. Mulik, D. P. Amalnerkar, "Electrochemically synthesised conducting polymeric materials for applications towards technology in electronics, optoelectronics and energy storage devices" *Materials Chemistry and Physics*, vol. 61, pp. 173-91, 1999.
- [96] S. Stafström, J. L. Brédass, "Electronic structure of highly conducting conjugated polymers: evolution upon doping of polyacetylene, polythiophene, and polyemeraldine" *Journal of Molecular Structure: THEOCHEM*, vol. 188, pp. 393-427, 1989.

- [97] R. Erlandsson, W. R. Salaneck, I. Lundström, "Electrically conducting organic polymer materials: Defects make them better" *Materials & Design*, vol. 7, pp. 246-251, 1986.
- [98] B. Malhotra, "Defects in conducting polymers" *Bulletin of Materials Science*, vol. 10, pp. 85-96, 1988.
- [99] H. Kaneko, Y. Nogami, T. Ishiguro, H. Nishiyama, H. Ishimoto, A. Takahashi, J. Tsukamoto, "Low temperature electrical conductivity of highly conducting iodine doped polyacetylene" *Synthetic Metals*, vol. 57, pp. 4888-4893, 1993.
- [100] C. K. Chiang, C. R. Fincher, Y. W. Park, A. J. Heeger, H. Shirakawa, E. J. Louis, S. C. Gau, A. G. MacDiarmid, "Electrical conductivity in doped polyacetylene" *Physical Review Letters*, vol. 39, pp. 1098 LP - 1101, 1977.
- [101] Y. W. Park, C. Park, Y. S. Lee, C. O. Yoon, H. Shirakawa, Y. Suezaki, K. Akagi, "Electrical conductivity of highly-oriented-polyacetylene" *Solid State Communications*, vol. 65, pp. 147-150, 1988.
- [102] J. P. Zheng and T. R. Jow, "High Energy and High Power Density Electrochemical Capacitors", *Journal of Power Sources*, vol. 62, pp. 155, 1996.
- [103] R. Taylor, H. Marsh, E.A. Heintz and F. Rodriguez, "Introduction to Carbon Technologies", *Universidad de Alcantre, Secretarido de Publicaciones*, pp. 167, 1997.
- [104] J. B. Donnet, R. C. Bansal and M. J. Wang, "Carbon Black Science and Technology", 2nd Ed., *Marcel Dekker, New York*, 1993.
- [105] R. Richner, S. Muller and A. Wokaum, "Crafted and Crosslinked Carbon Black as an Electrode Material for Double Layer Capacitors", *Carbon*, vol. 40, pp. 307, 2002.
- [106] C. C. Hu and C. C. Wang, "Effects of Electrolytes and Electrochemical PreTreatments on the Capacitive Characteristics of Activated Carbon Fabrics of Supercapacitors", *Journal of Power Sources*, vol. 125, pp. 299, 2004.

- [107] F. Beck, M. Dolata, E. Grivei and N. Probst, “Electrochemical Supercapacitors Based on Industrial Carbon Blacks in Aqueous H_2SO_4 ”, *Journal of Applied Electrochemie*, vol. 31, pp. 845, 2001.
- [108] J. Li, X. Wang, Q. Huang, S. Gamboa and P. J. Sebastian, “Studies on preparation and performances of carbon aerogel electrodes for the application of supercapacitor”, *Journal of Power Sources*, vol. 158, pp.786, 2006.
- [109] E. Frackowiak and F. Beguin, “Carbon Materials for the Electrochemical Storage of Energy in Capacitors”, *Carbon*, vol. 39, pp. 937, 2001.